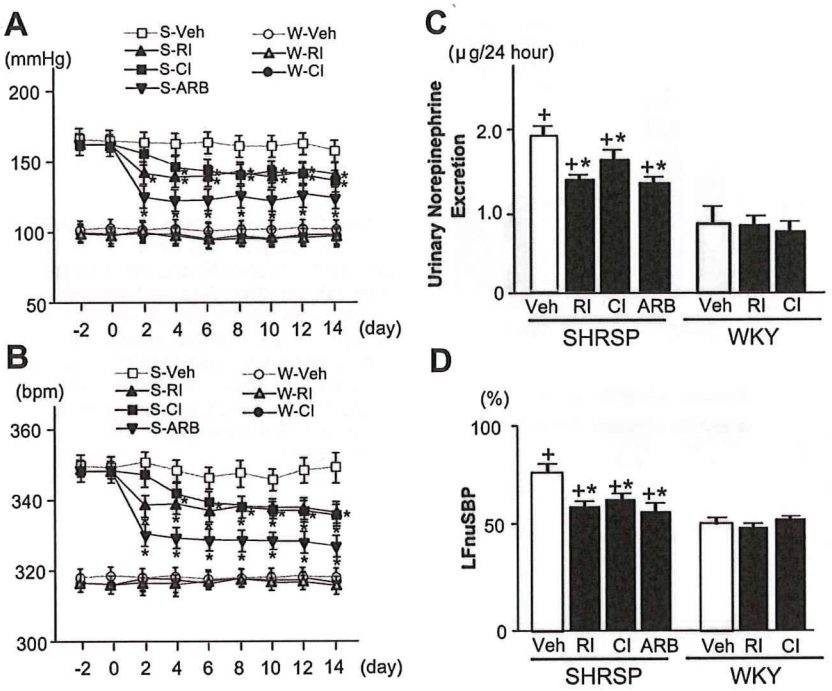

Figure 1. Time course of MBP (A, mm Hg) and HR (B, bpm) in S-RI (n=5), S-CI (n=5), S-ARB (n=5), S-Veh (n=5), W-RI (n=5), W-CI (n=5), and W-Veh (n=5). *P<0.05 for Ras inhibitor (RI), caspase-3 inhibitor (CI), or ARB vs vehicle (Veh) values in each strain. C and D, 24-hour uNE (μg) (C) and LFnuSBP (%) (D) on day 14 in SHRSP treated with RI, caspase-3 inhibitor (CI), ARB, or vehicle (Veh) and WKY treated with RI, caspase-3 inhibitor (CI), or Veh (n=5 for each). *P<0.05 for RI, CI, or ARB vs Veh values in each strain. +P<0.05 vs W-Veh. Data are shown as mean±SEM.

S-RI than in S-Veh (Figure 4A through 4C). ICV infusion of Z-DEVD-FMK significantly inhibited caspase-3 activity in both SHRSP and WKY (Figure 4A). In WKY, however, neither caspase-3 activity nor the expression of Bax and Bad differed between W-Veh and W-RI (Figure 4A through 4C). ICV infusion of candesartan in SHRSP significantly decreased caspase-3 activity and the expression of Bax and Bad (Figure 4A through 4C).

The expression of Bcl-2 was significantly lower in S-Veh than in W-Veh (Figure 4D) and significantly higher in S-RI than in S-Veh (Figure 4D). In WKY, however, the expression of Bcl-2 did not differ between W-Veh and W-RI (Figure 4D). ICV infusion of candesartan in SHRSP significantly increased Bcl-2 expression (Figure 4D).

Microinjection of Angiotensin II into the RVLM

The changes in MBP, HR, and LFnuSBP evoked by microinjection of angiotensin II into the bilateral RVLM were significantly smaller in S-RI than in S-Veh (MBP, 8±5 mm Hg versus 14±3 mm Hg; HR, 7±8 bpm versus 22±9 bpm; LFnuSBP, 3±3% versus 8±2%; n=5 for each; P<0.01).

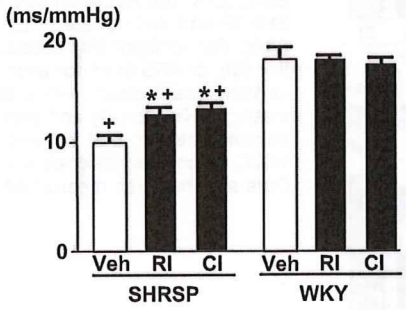

Figure 2. BRS (ms/mm Hg) in SHRSP and WKY treated with vehicle (Veh), Ras inhibitor (RI), or caspase-3 inhibitor (CI) (n=5 for each). *P<0.05 vs Veh in each strain. +P<0.05 vs W-Veh. Data are shown as mean±SEM.

Discussion

The novel findings in the present study are as follows: (1) Ras, p38 MAPK, ERK, mitochondrial apoptotic proteins Bax and Bad, and caspase-3 in the RVLM are activated in SHRSP; (2) ICV infusion of a Ras inhibitor decreases MBP, HR, and SNA and increases BRS through the partial inhibition of p38 MAPK, ERK, Bax, Bad, and caspase-3 in the RVLM of SHRSP; (3) ICV infusion of a caspase-3 inhibitor decreases MBP, HR, and SNA and increases BRS through the partial inhibition of caspase-3 in the RVLM of SHRSP; (4) ICV infusion of candesartan decreases systolic blood pressure, HR, and SNA through the partial inhibition of Ras, p38 MAPK, ERK, Bax, Bad, and caspase-3 in the RVLM of SHRSP; and (5) ICV infusion of the Ras inhibitor in SHRSP abolishes the pressor effect evoked by the microinjection of angiotensin II into the RVLM. These findings indicate that AT_1R-induced activation of caspase-3 through the Ras/p38 MAPK/ERK pathway in the RVLM might increase MBP, HR, and SNA and decrease BRS (Figure 5).

The present findings are the first to demonstrate that Ras, p38 MAPK, and ERK activity is increased in the RVLM of SHRSP. A previous study suggested that an acute injection of angiotensin II induced AT_1R-dependent ROS production and phosphorylation of p38 MAPK and ERK in the RVLM.[27] Activation of p38 MAPK and ERK by angiotensin II is also reported in mesenteric smooth muscle cells[33,34] and aorta.[35,36] In the forebrain, MAPK is activated in a model of heart failure in which the brain renin-angiotensin system is upregulated.[37] ROS activates Ras,[38] and Ras activates caspase-3 through p38 MAPK and ERK.[4–7,39] Previously, we demon-

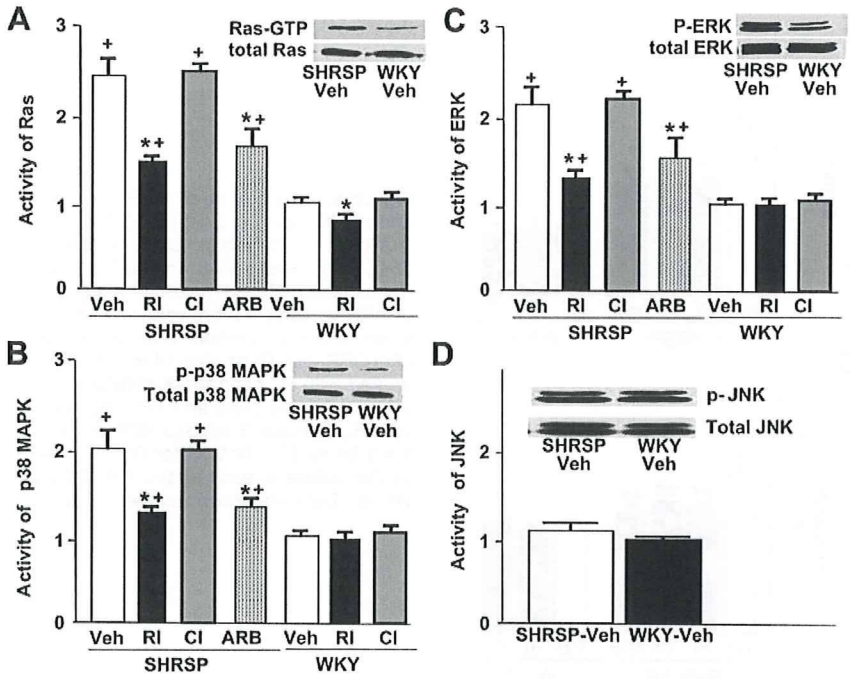

Figure 3. Activity of Ras (A), p38 MAPK (B), ERK (C), and JNK (D) in the RVLM on day 14 in SHRSP and WKY treated with vehicle (Veh), Ras inhibitor (RI), caspase-3 inhibitor (CI), or ARB (n=5/group). *$P<0.05$ vs Veh in each strain. +$P<0.05$ vs Veh-treated WKY. Activity is expressed relative to that in Veh-treated WKY, which was assigned a value of 1. Data are shown as mean±SEM.

strated that ROS in the RVLM increases SNA,[20,22] and ROS is produced in the brain by angiotensin II and NAD(P)H oxidase.[25] In the present study, ICV infusion of the Ras inhibitor decreased MBP, HR, and SNA and increased BRS because of the partial inhibition of Ras, p38 MAPK, ERK, and caspase-3 in the RVLM of SHRSP, and it abolished the pressor effect evoked by the microinjection of angiotensin II into the RVLM. ICV infusion of the caspase-3 inhibitor also inhibited MBP, HR, and SNA and increased BRS through the partial inhibition of caspase-3 activity in the RVLM of SHRSP. Furthermore, ICV infusion of candesartan decreased MBP, HR, and SNA, consistent with previous reports.[32] In the present study, ICV infusion of candesartan also partially inhibited Ras, p38 MAPK, ERK, and caspase-3 in the RVLM of SHRSP. The degree of the depressor effect of the Ras inhibitor on MBP in SHRSP was almost half that in WKY. These results suggest that AT_1R-activated caspase-3 acting through the Ras/MAPK/ERK pathway in the RVLM is one of the major pathways through which MBP, HR, and SNA are increased and BRS is decreased in SHRSP.

Another intriguing finding of the present study is that the apoptotic proteins Bax and Bad were activated, and the

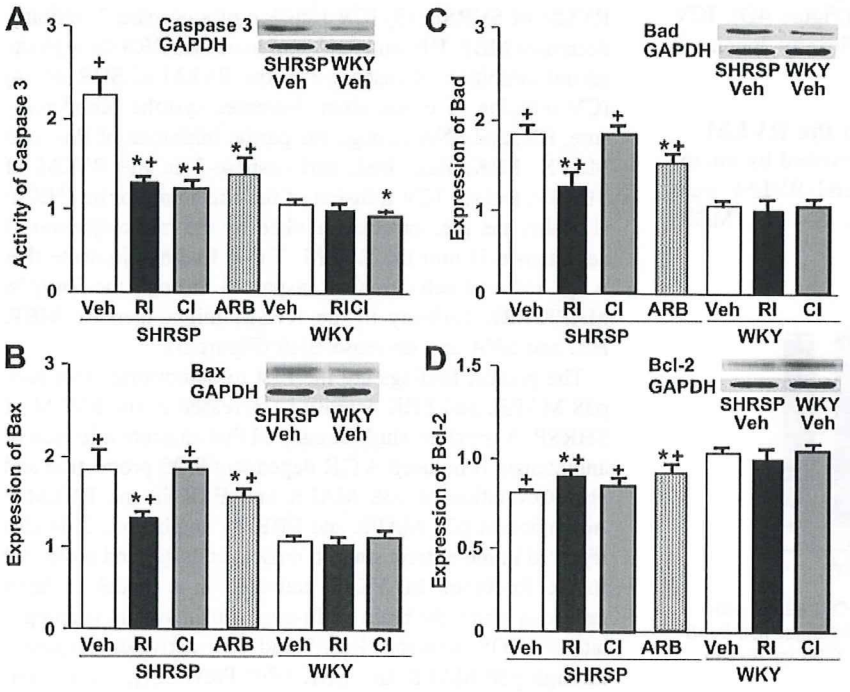

Figure 4. Activity of caspase-3 (A) and expression of Bax (B), Bad (C), and Bcl-2 (D) in the RVLM on day 14 in SHRSP and WKY treated with vehicle (Veh), Ras inhibitor (RI), caspase-3 inhibitor (CI), or ARB (n=5 for each). *$P<0.05$ vs Veh in each strain. +$P<0.05$ vs Veh-treated WKY. Activity and expression are shown relative to that in Veh-treated WKY, which was assigned a value of 1. Data are shown as mean±SEM.

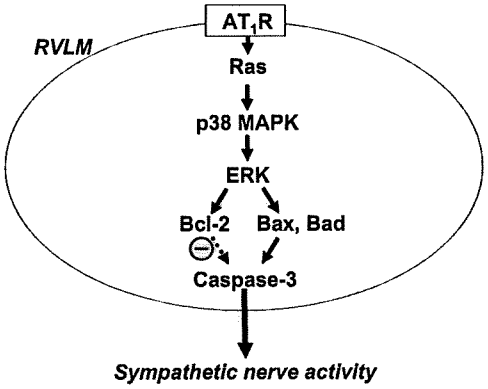

Figure 5. Illustration showing the major findings suggested by the results of the present study.

antiapoptotic protein Bcl-2 was inhibited in the RVLM of SHRSP. Neuronal apoptosis is mediated by caspase-3 activated by Bax and Bad and inhibited by Bcl-2 in mitochondria.[1] Activation of caspase-3 induces neuronal apoptosis.[18,19] Other reports indicate that p38 MAPK and ERK activate caspase-3–dependent neuronal apoptosis.[8] We previously demonstrated that mitochondria-derived ROS mediate sympathoexcitation induced by angiotensin II in the RVLM,[40] and these results suggest that mitochondrial dysfunction in the RVLM causes sympathoexcitation via ROS production. We hypothesized that Ras, p38 MAPK, and ERK activate the mitochondrial apoptotic pathway and inhibit the mitochondrial antiapoptotic pathway and that caspase-3–dependent neuronal apoptosis is activated in the RVLM of SHRSP. The possibility of caspase-3–independent neuronal apoptosis in the RVLM or of a direct link between ROS and caspase-3 activation was not examined in the present study. A previous report suggested that neural apoptosis in the RVLM leads to a reduction of sympathetic outflow.[40] Further study is necessary to determine the reasons for this discrepancy.

In the present study, we determined the ICV infusion dose of the Ras or caspase-3 inhibitor that inhibits blood pressure, HR, and SNA. There were dose-dependent effects of the Ras and caspase-3 inhibitors on blood pressure and HR (data not shown). Furthermore, the doses of Ras or caspase-3 inhibitor used in the present study did not change blood pressure or HR when injected intravenously (data not shown). In addition, Ras and caspase-3 activity were significantly higher in SHRSP than in WKY, and the depressor and sympathoinhibitory effects of Ras and caspase-3 inhibitors were also significantly greater in SHRSP than in WKY. Thus, we consider that the doses of Ras and caspase-3 inhibitor used in the present study were reasonable to inhibit Ras or caspase-3 activity in the RVLM. Future studies, however, are needed to investigate the effects of inhibiting Ras or caspase-3 activity specifically in the RVLM.

Interestingly, JNK was not altered in the RVLM of SHRSP. JNK is an upstream activator of apoptosis. In a heart failure model, JNK is upregulated in the RVLM.[41] Angiotensin II and NAD(P)H oxidase-derived superoxide anions, however, do not activate JNK in the RVLM,[27] and these findings are consistent with the present results. We did not explore the mechanisms of this discrepancy in the present study and are therefore not able to exclude the importance of JNK in the RVLM for cardiovascular regulation. JNK in the RVLM might be significantly activated in heart failure progressing to hypertension. Furthermore, we did not examine the protein kinase C–dependent pathway in the RVLM. A previous report indicates that protein kinase C–dependent translocation of Bax in the RVLM initiates caspase-3–dependent apoptosis during experimental endotoxemia.[28] It is possible that this pathway is also a major pathway involved in the increase in SNA in SHRSP.

The present study has some limitations. Ras activity in the RVLM was inhibited by ICV infusion of the Ras inhibitor, and the inhibition of Ras activity was not limited to the RVLM; therefore, we cannot exclude the possible effects of Ras inhibition in other brain sites, and our results do not suggest that the AT_1R/Ras/caspase-3 pathway in the RVLM is the only major pathway of the sympathetic control. Moreover, none of the ICV antagonists completely normalized BP, HR, and SNA in SHRSP. Many factors in the RVLM may be involved in changing SNA. Nevertheless, Ras activity was inhibited in the RVLM, and, therefore, the neural activity of the RVLM directly influenced SNA.[23,24] Furthermore, we found that the pressor effect evoked by microinjection of angiotensin II into the RVLM was attenuated in SHRSP treated with ICV infusion of the Ras inhibitor. Previous reports suggest that activation of the brain angiotensin system contributes to the neural mechanisms of hypertension.[23,24,42–45] In addition, a renin-angiotensin system also exists inside the blood-brain barrier.[42,46] All components of the renin-angiotensin system are present in the brain, such as renin, angiotensinogen, angiotensin-converting enzyme, angiotensin II, and AT_1 and angiotensin type 2 (AT_2) receptors.[45] Importantly, AT_1 receptors are richly distributed in the paraventricular nucleus of the hypothalamus, nucleus tractus solitarius, and RVLM, which are involved in autonomic cardiovascular regulation.[42,44–46] Therefore, it is conceivable that alteration of a signaling pathway in the RVLM influences central sympathetic outflow via AT_1R in the RVLM of SHRSP, although we cannot exclude the possible interaction of other autonomic nuclei, such as the paraventricular nucleus of the hypothalamus. The findings of the present study do not exclude the possibility that similar effects might occur in other nuclei or that these findings are indirect effects. In this regard, further study is necessary to determine the role of other autonomic nuclei in neural control of blood pressure. It would be interesting if we could examine the direct effect of chronic infusion of a Ras inhibitor and/or a caspase inhibitor directly into the RVLM. In addition, we did not measure SNA directly in the present study because chronic direct measurement of SNA is technically difficult. We examined SNA by measuring 24-hour uNE and spectral analysis of systolic blood pressure. uNE is considered to be a measure of SNA,[20,47] and measurement of uNE is often used to assess SNA in small awake animals.[47] We consider that uNE and LFnuSBP are appropriate parameters for assessing SNA.

In conclusion, AT_1R-induced activation of caspase-3 through Ras/p38 MAPK/ERK and the mitochondrial apoptotic pathway in the RVLM of SHRSP increases blood pressure, HR, and SNA

and decreases BRS in SHRSP. Inhibition of this pathway by ARB in the RVLM may be a novel therapeutic approach to sympathoexcitation in hypertension.

Perspectives

Our results suggest that Ras-activated caspase-3, acting through the p38 MAPK, ERK, and mitochondrial apoptotic pathways in the RVLM, increases SNA. Previous studies indicate that angiotensin II and ROS produced by NAD(P)H oxidase are upstream of Ras. In the RVLM, angiotensin II and ROS are important modulating factors regulating SNA, which is involved in cardiovascular disease, such as hypertension and heart failure. We consider that neural apoptosis in the RVLM is a novel target for the treatment of cardiovascular diseases exhibiting increased SNA.

Acknowledgments

Candesartan was kindly provided by Takeda Co., Ltd.

Sources of Funding

This study was supported by a Grant-in-Aid for Scientific Research from the Japan Society for the Promotion of Science (B193290231) and in part by a Kimura Memorial Foundation Research Grant and Takeda Science Foundation.

Disclosures

None.

References

1. Buss RR, Oppenheim RW. Role of programmed cell death in normal neuronal development and function. *Anat Sci Int.* 2004;79:191–197.
2. Lossi L, Merighi A. In vivo cellular and molecular mechanisms of neuronal apoptosis in the mammalians CNS. *Prog Neurobiol.* 2003;69: 287–312.
3. De Zio D, Giunta L, Corvaro M, Ferraro E, Cecconi F. Expanding roles of programmed cell death in mammalian neurodevelopment. *Semin Cell Dev Biol.* 2005;16:281–294.
4. Griendling KK, Sorescu D, Lassegue B, Ushio-Fukai M. Modulation of protein kinase activity and gene expression by reactive oxygen species and their role in vascular physiology and pathophysiology. *Arterioscler Thromb Vasc Biol.* 2000;20:2175–2183.
5. Pearson G, Robinson F, Beers Gibson T, Xu BE, Karandikar M, Berman K, Cobb MH. Mitogen-activated protein kinase pathways; regulation and physiological functions. *Endocr Rev.* 2001;22:153–183.
6. Mielke K, Herdegen T. JNK and p38 stress kinase-degenerative effectors of signal-transduction-cascade in the nervous system. *Prog Neurobiol.* 2000;61:45–60.
7. Harper SJ, LoGrasso P. Signalling for survival and death in neurons: the role of stress-activated kinases, JNK and p38. *Cell Signal.* 2001;13: 299–310.
8. Cheng A, Chan SL, Milhavet O, Wang S, Mattson MP. p38 MAP kinase mediates nitric oxide-induced apoptosis of neural progenitor cells. *J Biol Chem.* 2001;276:43320–43327.
9. Hunter T. Oncoprotein networks. *Cell.* 1997;88:333–346.
10. Lloyd AC, Obermuller F, Staddon S, Barth CF, McMahon M, Land H. Cooperating oncogenes converge to regulate cyclin/cdk complexes. *Genes Dev.* 1997;11:663–677.
11. Serrano M, Lin AW, McCurrach ME, Beach D, Lowe SW. Oncogenic ras provokes premature cell senescence associated with accumulation of p53 and p16INK4a. *Cell.* 1997;88:593–602.
12. Shao J, Sheng H, DuBois RN, Beauchamp RD. Oncogenic Ras-mediated cell growth arrest and apoptosis are associated with increased ubiquitin-dependent cyclin D1 degradation. *J Biol Chem.* 2000;275:22916–22924.
13. Chen CY, Liou J, Forman LW, Faller DV. Differential regulation of discrete apoptotic pathways by Ras. *J Biol Chem.* 1998;273:16700–16709.
14. Nesterov A, Nikrad M, Johnson T, Kraft AS. Oncogenic Ras sensitizes normal human cells to tumor necrosis factor-alpha related apoptosis-inducing ligand-induced apoptosis. *Cancer Res.* 2004;64:3922–3927.
15. Downward J. PI 3-kinase, Akt and cell survival. *Semin Cell Dev Biol.* 2004;15:177–182.
16. Choi JA, Park MT, Kang CM, Um HD, Bae S, Lee KH, Kim TH, Kim JH, Cho CK, Lee YS, Chung HY, Lee SJ. Opposite effects of Ha-Ras and Ki-Ras on radiation-induced apoptosis via differential activation of PI3K/Akt and Rac/p38 mitogen-activated protein kinase signaling pathways. *Oncogene.* 2004;23:9–20.
17. Predescu SA, Predescu DN, Knezevic I, Klein IK, Malik AB. Intersectin-1s regulates the mitochondrial apoptotic pathway in endothelial cells. *J Biol Chem.* 2007;282:17166–17178.
18. Earnshaw WC, Martins LM, Kaufmann SH. Mammalian caspases: structure, activation, substrates, and functions during apoptosis. *Annu Rev Biochem.* 1999;68:383–424.
19. Baydas G, Reiter RJ, Akbulut M, Tuzcu M, Tamer S. Melatonin inhibits neural apoptosis induced by homocysteine in hippocampus of rats via inhibition of cytochrome c translocation and caspase-3 activation and by regulating pro- and anti-apoptotic protein levels. *Neuroscience.* 2005;135: 879–886.
20. Kishi T, Hirooka Y, Kimura Y, Ito K, Shimokawa H, Takeshita A. Increased reactive oxygen species in rostral ventrolateral medulla contribute to neural mechanisms of hypertension in stroke-prone spontaneously hypertensive rats. *Circulation.* 2004;109:2357–2362.
21. Peterson JR, Sharma RV, Davisson RL. Reactive oxygen species in the neuropathogenesis of hypertension. *Curr Hypertens Rep.* 2006;8: 232–241.
22. Hirooka Y. Role of reactive oxygen species in brainstem in neural mechanisms of hypertension. *Auton Neurosci.* 2008;142:20–24.
23. Dampney RA, Coleman MJ, Fontes MA, Hirooka Y, Horiuchi J, Li YW, Polson JW, Potts PD, Tagawa T. Central mechanisms underlying short- and long-term regulation of the cardiovascular system. *Clin Exp Pharmacol Physiol.* 2002;29:261–268.
24. Guyenet PG. The sympathetic control of blood pressure. *Nat Rev Neurosci.* 2006;7:335–346.
25. Okamoto K, Aoki K. Development of a strain of spontaneously hypertensive rats. *Jpn Circ J.* 1963;27:282–293.
26. Zimmerman MC, Dunlay RP, Lazartigues E, Zhang Y, Sharma RV, Engelhardt JF, Davisson RL. Requirement for Rac1-dependent NADPH oxidase in the cardiovascular and dipsogenic actions of angiotensin II in the brain. *Circ Res.* 2004;95:532–539.
27. Chan SH, Hsu KS, Huang CC, Wang LL, Ou CC, Chan JY. NADPH oxidase-derived superoxide anion mediates angiotensin II-induced pressor effect via activation of p38 mitogen-activated protein kinase in the rostral ventrolateral medulla. *Circ Res.* 2005;97:772–780.
28. Chan JY, Chang AY, Wang LL, Ou CC, Chan SH. Protein kinase c-dependent mitochondrial translocation of proapoptotic protein Bax on activation of inducible nitric oxide synthase in rostral ventrolateral medulla mediates cardiovascular depression during experimental endotoxemia. *Mol Pharmacol.* 2007;71:1129–1139.
29. Braga VA, Burmeister MA, Sharma RV, Davisson RL. Cardiovascular responses to peripheral chemoreflex activation and comparison of different methods to evaluate baroreflex gain in conscious mice using telemetry. *Am J Physiol.* 2008;295:R1168–R1174.
30. Goldberg L, Haklai R, Bauer V, Heiss A, Kloog Y. New derivatives of farnesylthiosalicylic acid (salirasib) for cancer treatment: farnesylthiosalicylamide inhibits tumor growth in nude mice models. *J Med Chem.* 2009;52:197–205.
31. Stepanichev MY, Kudryashova IV, Yakovlev AA, Onufriev MV, Khaspekov LG, Lyzhin AA, Lazareva NA, Gulyaeva NV. Central administration of a caspase inhibitor impairs shuttle-box performance in rats. *Neuroscience.* 2005;136:579–591.
32. Yamazato M, Ohya Y, Nakamoto M, Sakima A, Tagawa T, Harada Y, Nabika T, Takishita S. Sympathetic hyperreactivity to air-jet stress in the chromosome 1 blood pressure quantitative trait locus congenic rats. *Am J Physiol.* 2006;290:R709–R714.
33. Touyz RM, He G, El Mabrouk M, Diep Q, Mardigyan V, Schiffrin EL. Differential activation of extracellular signal-regulated protein kinase 1/2 and p38 mitogen activated-protein kinase by At1 receptors in vascular smooth muscle cells from Wister-Kyoto rats and spontaneously hypertensive rats. *J Hypertens.* 2001;19:553–559.
34. Viedt C, Soto U, Krieger-Brauer HI, Fei J, Elsing C, Kubler W, Kreuzer J. Differential activation of mitogen-activated protein kinase in smooth muscle cells by angotensin II: involvement of p22phox and reactive oxygen species. *Arterioscler Thromb Vasc Biol.* 2000;20: 940–948.

35. Touyz RM, Cruzado M, Tabet F, Yao G, Salomon S, Schiffrin EL. Redox-dependent AMP kinase signaling by Ang II in vascular smooth muscle cells: role of receptor tyrosine kinase transactivation. *Can J Physiol Pharmacol.* 2003;81:159–167.
36. Izumi Y, Kim S, Zhan Y, Namba M, Yasumoto H, Iwao H. Important role of angiotensin II-mediated c-Jun NH2-terminal kinase activation in cardiac hypertrophy in hypertensive rats. *Hypertension.* 2000;36: 511–516.
37. Zhang GX, Kimura S, Nishiyama A, Shokoji T, Rahman M, Abe Y. ROS during the acute phase of Ang II hypertension participates in cardiovascular MAPK activation but not vasoconstriction. *Hypertension.* 2004;43: 117–124.
38. Kuster GM, Siwik DA, Pimentel DR, Colucci WS. Role of reversible, thioredoxin-sensitive oxidative protein modifications in cardiac myocytes. *Antioxid Redox Signal.* 2006;8:2153–2159.
39. McDermott EP, O'Neill LA. Ras participates in the activation of p38 MAPK by interleukin-1 by associating with IRAK, IRAK2, TRAF6, and TAK-1. *J Biol Chem.* 2002;277:7808–7815.
40. Nozoe M, Hirooka Y, Koga Y, Araki S, Konno S, Kishi T, Ide T, Sunagawa K. Mitochondria-derived reactive oxygen species mediate sympathoexcitation induced by angiotensin II in the rostral ventrolateral medulla. *J Hypertens.* 2008;26:2176–2184.
41. Liu D, Gao L, Roy SK, Cornish KG, Zucker IH. Neuronal angiotensin II type 1 receptor upregulation in heart failure: activation of activator protein 1 and Jun N-terminal kinase. *Circ Res.* 2006;99:1004–1011.
42. Phillips MI, Sumners C. Angiotensin II in central nervous system physiology. *Regul Pept.* 1998;78:1–11.
43. Pilowsky PM, Goodchild AK. Baroreceptor reflex pathways and neurotransmitters: 10 years on. *J Hypertens.* 2002;20:1675–1688.
44. McKinley MJ, Albiston AL, Allen AM, Mathai ML, May CN, McAllen RM, Oldfield BJ, Mendelsohn FA, Chai SY. The brain renin-angiotensin system: location and physiological roles. *Int J Biochem Cell Biol.* 2003; 35:901–918.
45. Saavedra JM. Brain angiotensin II: new developments, unanswered questions and therapeutic opportunities. *Cell Mol Neurobiol.* 2005;25: 485–512.
46. Seltzer A, Bregonzio C, Armando I, Baiardi G, Saavedra JM. Oral administration of an AT1 receptor antagonist prevents the central effects of angiotensin II in spontaneously hypertensive rats. *Brain Res.* 2004; 1028:9–18.
47. Xie T, Plagge A, Gavrilova O, Pack S, Jou W, Lai EW, Frontera M, Kelsey G, Weinstein LS. The alternative stimulatory G protein α-subunit XLαs is a critical regulator of energy and glucose metabolism and sympathetic nerve activity in adult mice. *J Biol Chem.* 2006;281: 18989–18999.

Sympathoinhibition Induced by Centrally Administered Atorvastatin Is Associated With Alteration of NAD(P)H and Mn Superoxide Dismutase Activity in Rostral Ventrolateral Medulla of Stroke-Prone Spontaneously Hypertensive Rats

Takuya Kishi, MD, PhD, Yoshitaka Hirooka, MD, PhD, Satomi Konno, MD, and Kenji Sunagawa, MD, PhD

Abstract: Oxidative stress in the rostral ventrolateral medulla (RVLM) increases sympathetic nervous system activity (SNA). Oral treatment with atorvastatin decreases SNA through antioxidant effects in the RVLM of stroke-prone spontaneously hypertensive rats (SHRSP). We aimed to examine whether centrally administered atorvastain reduces SNA in SHRSP and, if so, to determine whether it is associated with the reduction of oxidative stress induced by alteration of activities of nicotinamide adenine dinucleotide phosphate [NAD(P)H] oxidase and superoxide dismutase (SOD) in the RVLM of SHRSP. SHRSP received atorvastatin (S-ATOR) or vehicle (S-VEH) by continuous intracerebroventricular infusion for 14 days. Mean blood pressure, heart rate, and SNA were significantly lower in S-ATOR than in S-VEH. Oxidative stress, Rac1 activity, NAD(P)H oxidase activity, Rac1, gp91^{phox} and p22^{phox} expression in the membrane fraction, and p47^{phox} and p40^{phox} expression in the cytosolic fraction in the RVLM were significantly lower in S-ATOR than in S-VEH. Rac1 expression in the cytosolic fraction and Mn-SOD activity, however, were significantly higher in S-ATOR than in S-VEH. Our findings suggest that centrally administered atorvastatin decreases SNA and is associated with decreasing NAD(P)H oxidase activity and upregulation of Mn-SOD activity in the RVLM of SHRSP, leading to suppressing oxidative stress.

Key Words: hypertension, sympathetic nerve activity, atorvastatin, oxidative stress, brain

(*J Cardiovasc Pharmacol*™ 2010;55:184–190)

INTRODUCTION

In the brainstem, the rostral ventrolateral medulla (RVLM) is known as one of the vasomotor centers that regulates sympathetic nervous system activity (SNA).[1,2] Previously, we reported that the levels of reactive oxygen species (ROS) in the RVLM are increased in stroke-prone spontaneously hypertensive rats (SHRSP), which is a hypertensive rat model exhibiting increased SNA. We also demonstrated that the increase in SNA was due to ROS activation,[3] consistent with the findings of other studies.[4–6] Furthermore, oral administration of atorvastatin, an inhibitor of 3-hydroxy-3-methylglutaryl coenzyme A reductase, suppresses SNA probably through the inhibition of ROS in the RVLM of SHRSP.[7] Other studies suggest that central infusion of simvastatin suppresses SNA in heart failure models.[8–10] Our previous study was based on the oral administration of atorvastatin, however, and it is not known whether atorvastatin directly and chronically administered into the brain reduces the central sympathetic outflow via its effects on oxidative stress in the brain, particularly in the RVLM of hypertensive models.

In the brain, ROS are produced mainly through the activation of nicotinamide adenine dinucleotide phosphate [NAD(P)H] oxidase by the small G protein Rac1.[11,12] NAD(P)H oxidase is a multicomponent enzyme complex that comprises a membrane-bound heterodimer of gp91^{phox} (phagocytic oxidase) and p22^{phox}, and the cytosolic regulatory subunits p40^{phox}, p47^{phox}, p67^{phox}, and Rac1.[13–15] Transfection of dominant-negative Rac1 in the nucleus tractus solitarius decreases ROS and SNA.[12] Atorvastatin is also suggested to inhibit NAD(P)H oxidase activity in the vasculature,[16] the quadriceps muscle of diabetic rats,[17] and cardiomyocytes.[18] Furthermore, atorvastatin inhibits membrane translocation of Rac1, which is required for the activation of NAD(P)H oxidase in the vasculature.[16] In the kidney, rosuvastatin attenuates NAD(P)H oxidase activity through the inhibition of Rac1 and p22^{phox}.[18,19] In the brain, however, the contribution of atorvastatin to reducing ROS and its involvement in the inhibition of the membrane translocation of Rac1 and NAD(P)H oxidase activity is unknown. We previously demonstrated that Mn superoxide dismutase (SOD) activity is decreased in the RVLM of SHRSP, and the decrease contributes to the increase

Received for publication September 7, 2009; accepted November 10, 2009.
From the Department of Cardiovascular Medicine, Kyushu University Graduate School of Medical Sciences, Fukuoka, Japan.
This study was supported by a Grant-in-Aid for Scientific Research from the Japan Society for the Promotion of Science (B19390231).
The authors report no conflicts of interest.
Reprints: Yoshitaka Hirooka, MD, PhD, FAHA, Department of Cardiovascular Medicine, Kyushu University Graduate School of Medical Sciences, 3-1-1 Maidashi, Higashi-ku, Fukuoka 812-8582, Japan (e-mail: hyoshi@cardiol.med.kyushu-u.ac.jp).

in ROS.[3] A number of reports suggest that statins upregulate SOD in the vasculature.[20–23] Furthermore, the upregulation of Rac1 and NAD(P)H oxidase and the inhibition of SOD in the RVLM and nucleus tractus solitarius have major roles in increasing SNA and blood pressure (BP).[3,24] However, the mechanisms involved by which atorvastatin reduces ROS in the RVLM of SHRSP are not evaluated. The aim of the present study was thus to determine whether the sympathoinhibitory effect of atorvastatin due to the reduction of ROS in the RVLM is caused by the inhibition of Rac1-NAD(P)H oxidase activity and upregulation of Mn-SOD and Cu/Zn-SOD in the RVLM of SHRSP. Therefore, the aim of the present study was to examine the effects of atorvastatin administered into the brain and evaluate the changes in BP and SNA in SHRSP and to evaluate the oxidative stress and the NAD(P)H oxidase activity in the RVLM as the ROS generation. For this purpose, we determined the expression of Rac1, gp91^{phox}, and p22^{phox} in the membrane fraction and the expression of Rac1 and p40^{phox} in the cytosolic fraction of the RVLM. In addition, the activity of Cu/Zn-SOD, and Mn-SOD as scavenging enzymes of ROS was measured in the RVLM of intracerebroventricular (ICV) atorvastatin–treated and vehicle-infused SHRSP and Wistar Kyoto (WKY) rats.

MATERIALS AND METHODS

Animals and General Procedures

Male SHRSP/Izm rats and age-matched WKY rats (14–16 weeks old) were obtained from SLC Japan, Hamamatsu, Japan. Rats were fed a standard diet, and each strain was divided into 4 groups (SHRSP treated with atorvastatin, S-ATOR; SHRSP treated with vehicle, S-VEH; WKY treated with atorvastatin, W-ATOR; and WKY treated with vehicle, W-VEH; n = 5 per group). Atorvastatin (Pfizer, Inc, New York, NY) was dissolved in dimethyl sulfoxide and further diluted in artificial cerebrospinal fluid for a final concentration of 40 μg/mL. Atorvastatin or dimethyl sulfoxide in artificial cerebrospinal fluid was infused at 1 μL/h for 14 days with an osmotic minipump (Alzet 1003D; Alza Scientific Products, Palo Alto, CA) into the left lateral ventricle of the brain (from bregma: anteroposterior, −0.8 mm; lateral, 1.5 mm; and depth, 3.5 mm). The flow rate of agents in ICV methods was determined to have the significant effect in brainstem.[25] In a preliminary experiment, this dose of atorvastatin did not affect BP and heart rate (HR) when administered intravenously. Food and tap water were available ad libitum throughout the study. BP and HR were measured using the UA-10 radio-telemetry system (Data Science International, Dallas, TX) as described previously.[3,26–28] Urinary norepinephrine excretion (uNE) for 24 hours was calculated as an indicator of SNA, as described previously.[3,25–27] In addition, spectral analysis was performed using an adaptive autoregressive model to provide power spectra for systolic BP (SBP). Low frequency power of SBP was computed by integrating the spectra between 0.04 and 0.15 Hz, and SNA is presented as the normalized unit of the low frequency component of SBP (LFnuSBP).[29–31] Baroreflex sensitivity (BRS) was measured using the spontaneous sequence method as a parameter of autonomic control. Sequence analysis was performed to detect sequences of 3 or more beats in which there was either an increase in SBP and pulse interval (up sequence) or a decrease in SBP and pulse interval (down sequence). BRS was estimated as the mean slope of the up and down sequences.[32–34] The RVLM was defined according to a rat brain atlas as described previously.[3,26–28] The study protocol was reviewed and approved by the Committee on the Ethics of Animal Experiments at the Kyushu University Graduate School of Medical Sciences and conducted according to the Guidelines for Animal Experiments of Kyushu University.

Measurement of TBARS

The RVLM tissues were homogenized, and thiobarbituric acid (0.3%) was added to the homogenate. The mixture was extracted with a mixture of distilled water and *n*-butanolpyridine (15:1) and centrifuged at 1600*g* for 10 minutes. The amount of thiobarbituric acid reactive substances (TBARS) was determined by absorbance measured at 532 nm, as described previously.[3,7]

Expression of Rac1, gp91^{phox}, and p22^{phox} in the Membrane Fraction and Rac1, p47^{phox} and p40^{phox} in the Cytosolic Fraction

Western blot analysis was used to determine the expression of Rac1 (Upstate Biotechnology, Lake Placid, NY),[12] gp91^{phox}, and p22^{phox} in the membrane fraction (Santa Cruz Biotechnology, Santa Cruz, CA), and the expression of Rac1, p47^{phox}, and p40^{phox} in the cytosolic fraction (Santa Cruz Biotechnology, Santa Cruz, CA) of the RVLM.

Activity of Rac1 in the RVLM

Rac1 activity can be monitored by its interaction with p21-activated kinase, which only occurs when Rac1 is active. We used a Rac1 Activation kit (Upstate Biotechnology, Lake Placid, NY) to evaluate Rac1 activity in the RVLM, as previously described.[12]

NAD(P)H Oxidase Activity

NAD(P)H-dependent superoxide production in the RVLM was measured using a lucigenin luminescence assay as described previously.[35,36] Quantification of NAD(P)H oxidase activity was expressed relative to that in WKY rats, which was assigned a value of 1.

Cu/Zn-SOD and Mn-SOD Activity in the RVLM

Cu/Zn-SOD or Mn-SOD activity was assayed by monitoring the inhibition of the rate of xanthine-mediated/xanthine oxidase–mediated reduction of cytochrome c (pH 7.4). To discriminate between Cu/Zn-SOD and Mn-SOD activities, the assay was also performed after incubation in the presence of KCN, which selectively inhibits the Cu/Zn-SOD isoform.[37] Cu/Zn- and Mn-SOD activities were expressed relative to those in vehicle-treated WKY rats, which were assigned a value of 1.

Microinjection of Apocynin Into the Bilateral RVLM

In other S-ATOR and S-VEH, (n = 5 for each) on day 14, the NAD(P)H oxidase inhibitor apocynin (1 nmol) was microinjected bilaterally into the RVLM, as described previously.[3]

Statistical Analysis

Normally distributed variables were expressed as mean ± SD. An unpaired *t* test was used to compare the differences between groups of normally distributed variables, and the Mann–Whitney *U* test was used to compare differences between groups of non–normally distributed variables. A 2-factor repeated-measures analysis of variance was used to compare differences between groups. Differences were considered to be statistically significant with a *P* value of less than 0.05.

RESULTS

BP, HR, SNA, and BRS

Mean BP (MBP) and HR were significantly decreased on day 4 after the administration of atorvastatin in S-ATOR. On day 14, MBP, HR, 24-hour uNE, and LFnuSBP were significantly higher in S-VEH than in W-VEH and lower in S-ATOR than in S-VEH (Fig. 1A–D). BRS was significantly lower in S-VEH than in W-VEH (12.8 ± 2.3 vs. 19.7 ± 1.8 ms/mm Hg, n = 5 for each; $P < 0.05$) and significantly higher in S-ATOR than in S-VEH (16.4 ± 1.6 vs. 12.8 ± 2.3 ms/mm Hg, n = 5 for each; $P < 0.05$). Mean BP, HR, 24-hour uNE, LFnuSBP, and BRS values did not significantly differ between W-ATOR and W-VEH (Fig. 1A–D).

Oxidative Stress Measured by TBARS Methods in the RVLM

Oxidative stress in the RVLM measured by the TBARS method was significantly lower in S-ATOR than in S-VEH (Fig. 2). Oxidative stress did not differ significantly between W-ATOR and W-VEH (Fig. 2).

Activity of NAD(P)H Oxidase and Rac1 in the RVLM

The activity of NAD(P)H oxidase was significantly lower in S-ATOR than in S-VEH (Fig. 3A). The activity of Rac1 was also significantly lower in S-ATOR than in S-VEH (Fig. 3B). NAD(P)H oxidase activity and Rac1 activity did not significantly differ between W-ATOR and W-VEH (Fig. 3A, B).

Expression of Rac1, gp91^{phox}, and p22^{phox} in the Membrane Fraction and Rac1, p47^{phox}, and p40^{phox} in the Cytosolic Fraction

The expression of Rac1, gp91^{phox}, and p22^{phox} in the membrane fraction was significantly lower in S-ATOR than in S-VEH (Fig. 4A–C). The expression of p47^{phox} and p40^{phox} in the cytosolic fraction was also significantly lower in S-ATOR than in S-VEH (Fig. 5B, C). The expression of Rac1 in the cytosolic fraction was significantly higher, however, in S-ATOR than in S-VEH (Fig. 5A). The expression of Rac1, gp91^{phox}, and p22^{phox} in the membrane fraction and the expression of Rac1, p47^{phox}, and p40^{phox} in cytosolic fraction did not differ significantly between W-ATOR and W-VEH (Figs. 4A–C, 5A–C).

Cu/Zn- and Mn-SOD Activity in the RVLM

Mn-SOD activity in the RVLM was significantly higher in S-ATOR than in S-VEH, but Cu/Zn-SOD activity did not significantly differ between S-ATOR and S-VEH (Fig. 6A, B).

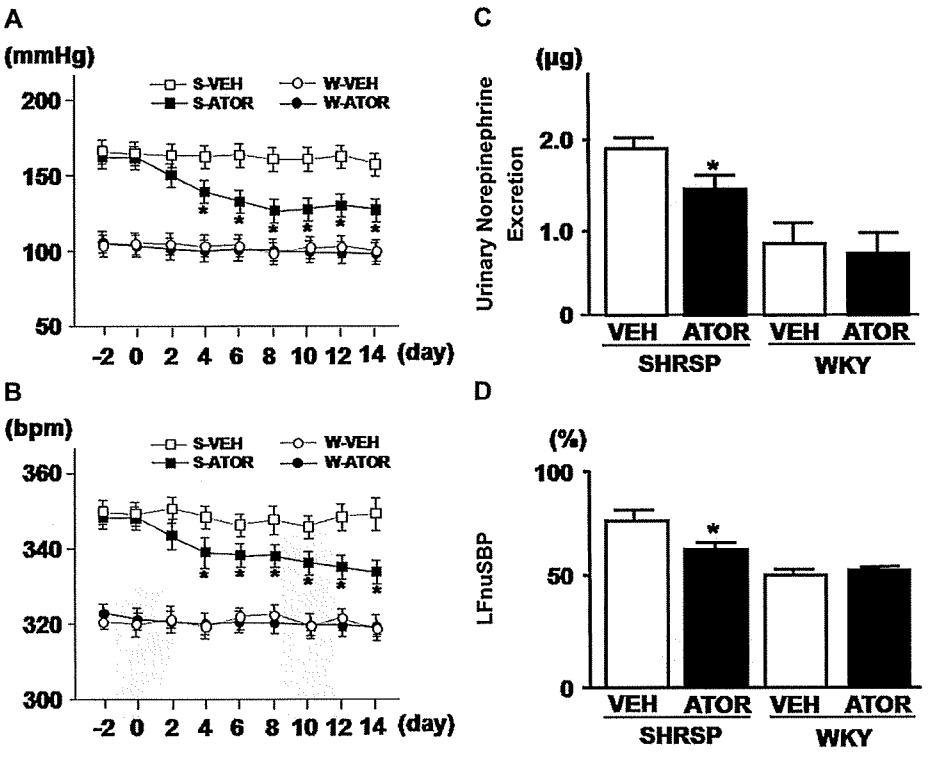

FIGURE 1. Time course of MBP (in mm Hg) (A) and HR (in beats per minute) (B) in S-ATOR (n = 5), S-VEH (n = 5), W-ATOR (n = 5), and W-VEH (n = 5). *$P < 0.05$ for ATOR versus VEH values in each strain. C, D, Urinary norepinephrine excretion for 24 hours (in micrograms) (C) and LFnuSBP (percentage) (D) at day 14 in ATOR- or VEH-treated SHRSP or WKY (n = 5 for each). *$P < 0.05$ for ATOR versus VEH values in each strain. †$P < 0.05$ compared with VEH-treated WKY. Data are shown as mean ± standard error of the mean.

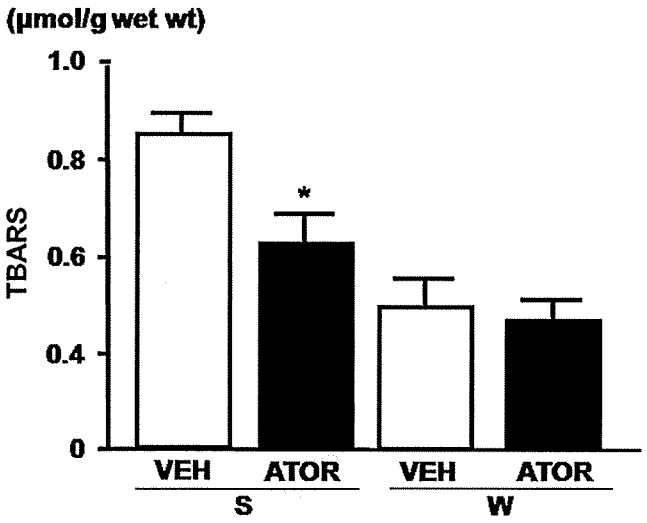

FIGURE 2. TBARS levels (in micromolars per gram wet weight) in the RVLM at day 14 in ATOR- or VEH-treated SHRSP or WKY (n = 5 for each). *$P < 0.05$ for ATOR versus VEH in each strain. †$P < 0.05$ compared with VEH-treated WKY. Data are shown as mean ± standard error of the mean.

Cu/Zn- and Mn-SOD activity did not significantly differ between W-ATOR and W-VEH (Fig. 6A, B).

Microinjection of Apocynin Into the RVLM

The degree of the change in MBP induced by the microinjection of apocynin into the bilateral RVLM was significantly smaller in S-ATOR than in S-VEH (−9.4 ± 1.9 vs. −26.4 ± 3.7 mm Hg; n = 5; $P < 0.05$).

DISCUSSION

The novel finding of the present study was that atorvastatin administered chronically into the brain in SHRSP reduced BP and SNA in SHRSP and that it was associated with reduced oxidative stress, probably due to the inhibition of NAD(P)H oxidase and the activation of Mn-SOD in the RVLM of SHRSP. This is supported by the following findings: (1) ICV injection of atorvastatin for 14 days decreased MBP, HR, SNA, and TBARS in the RVLM of SHRSP; (2) ICV injection of atorvastatin decreased NAD(P)H oxidase activity through the inhibition of Rac1 membrane translocation in the RVLM of SHRSP; (3) ICV injection of atorvastatin activated Mn-SOD in the RVLM of SHRSP; and (4) changes in MBP induced by microinjection of NAD(P)H oxidase inhibitor into the RVLM were significantly smaller in SHRSP treated with atorvastatin than in SHRSP treated with vehicle. Thus, atorvastatin inhibits Rac1 membrane translocation and Rac1 activity in the RVLM of SHRSP.

Atorvastatin decreased the expression of NAD(P)H membrane-bound subunits $gp91^{phox}$ and $p22^{phox}$ and the cytosolic regulatory subunit $p47^{phox}$ and $p40^{phox}$ and inhibited NAD(P)H oxidase activity in the RVLM of SHRSP. Oral administration of atorvastatin decreases ROS in the RVLM of SHRSP.[3] In the brain, ROS is produced mainly by NAD(P)H oxidase, which is activated through Rac1 membrane translocation.[11] In another area of the brainstem, the nucleus tractus solitarius, the inhibition of Rac1 decreases NAD(P)H oxidase activity and ROS formation.[12] Previous reports suggest that atorvastatin inhibits Rac1 membrane translocation and NAD(P)H oxidase activity in the vasculature of hypertensive rats.[13] We found that the depressor response elicited by apocynin into the RVLM was attenuated in SHRSP treated with ICV atorvastatin in the present study. Based on these findings, we suggest that the atorvastatin-induced reduction of ROS in the RVLM of SHRSP is caused by a decrease in NAD(P)H oxidase activity linked to the inhibition of Rac1 membrane translocation.

Atorvastatin activated Mn-SOD activity in the RVLM of SHRSP but not Cu/Zn-SOD. In the RVLM of SHRSP, Mn-SOD activity is decreased, and overexpression of Mn-SOD in the RVLM of SHRSP decreases ROS.[3] A number of reports suggest that statins activate total SOD[20–23] and Cu/Zn-SOD in the vasculature.[26,27] In the present study, however, atorvastatin did not activate Cu/Zn-SOD in the RVLM of SHRSP. In the nucleus tractus solitarius, Cu/Zn-SOD expression is decreased in SHRSP.[26] It is not clear why atorvastatin did not activate Cu/Zn-SOD in the present study. Recently, we reported that angiotensin II increases the intracellular Ca^{2+} concentration and that the increase in mitochondrial Ca^{2+} uptake leads to mitochondrial ROS production in the RVLM.[24] Therefore, it is possible that atorvastatin-induced activation of Mn-SOD in the RVLM of SHRSP contributes to inhibit ROS to an even greater extent than Cu/Zn-SOD.

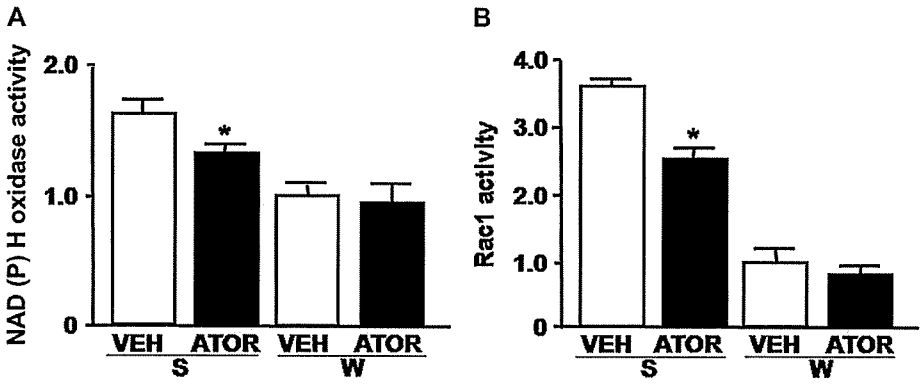

FIGURE 3. NAD(P)H oxidase activity (A) and Rac1 activity (B), in the RVLM at day 14 in ATOR- or VEH-treated SHRSP or WKY (n = 5 for each). *$P < 0.05$ for ATOR versus VEH in each strain. †$P < 0.05$ compared with VEH-treated WKY. NAD(P)H oxidase or Rac1 activity was expressed relative to that in W-VEH, which was assigned a value of 1. Data are shown as mean ± standard error of the mean.

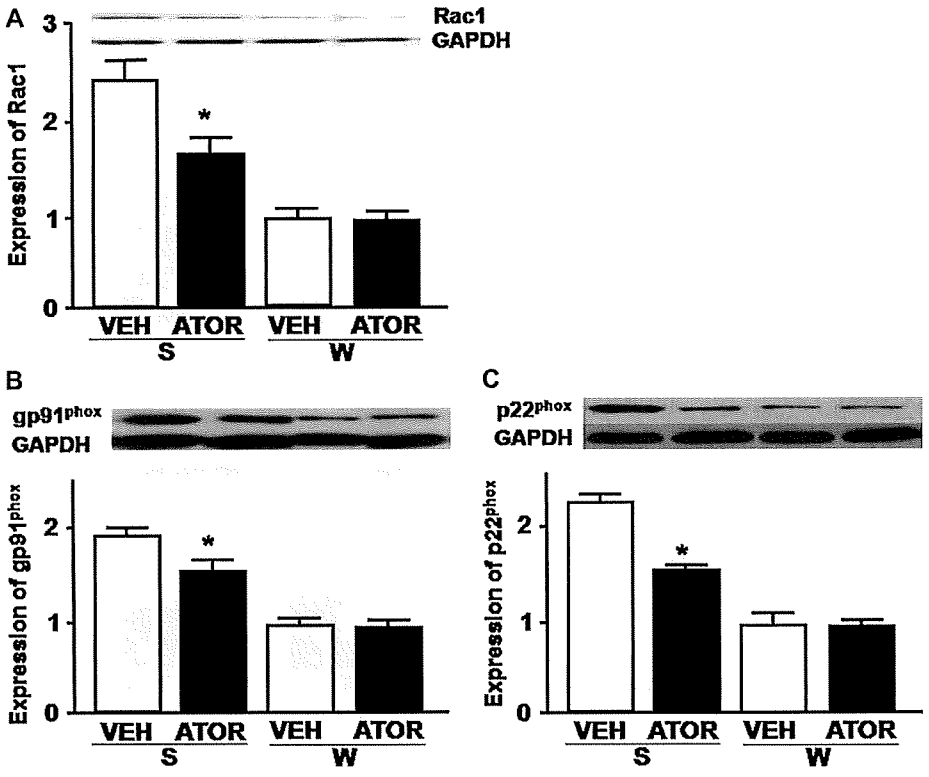

FIGURE 4. Western blot analysis showing the level of expression of Rac1 (A), gp91^{phox} (B), and p22^{phox} (C) in the membrane fraction of the RVLM at day 14 in ATOR- or VEH-treated SHRSP or WKY (n = 5 for each). *$P < 0.05$ for ATOR versus VEH in each strain. †$P < 0.05$ compared with VEH-treated WKY. The expression level of Rac1, gp91^{phox}, and p22^{phox} was expressed relative to that in W-VEH, which was assigned a value of 1. Data are shown as mean ± standard error of the mean.

In the present study, we measured SNA by spectral analysis. Low frequency power of SBP was computed by integrating the spectra between 0.04 and 0.15 Hz, and SNA is presented as LFnuSBP, as described in previous reports.[29–31] On day 14, the LFnuSBP values were comparable to those of uNE. Therefore, this method seems to be useful for measuring SNA in awake animals. Furthermore, atorvastatin improved the impaired baroreflex control in the SHRSP in the present study. Whereas we did not measure cardiac output in the present study and the reduction of BP and HR due to atorvastatin might cause a potential fall in cardiac output, the effects of atorvastatin are due to the decrease in sympathetic nerve activity. It is generally accepted that SNA is enhanced in SHRSP,[3,5,26–28,40] and atorvastatin attenuates the enhanced central sympathetic outflow to various organs including heart, kidney, and vasculature. At least, atorvastatin did not induce heart failure due to low cardiac output. We consider that the decrease in central sympathetic outflow reduced the peripheral vascular resistance by which cardiac output keep constant instead of the reduction of sympathetic outflow to the heart.

Another intriguing finding of the present study is that the BP-lowering and sympathoinhibitory effects are comparable between oral administration (50 mg/kg^{-1}/day^{-1})[7] and ICV injection (2 μg/kg^{-1}/day^{-1}) of atorvastatin. We confirmed the direct effects of atorvastatin administered into the brain on BP, SNA, and baroreflex function in SHRSP as one of the hypertensive models in the present study. The changes in TBARS levels are also similar between oral administration and ICV injection of atorvastatin. In SHRSP, the blood–brain barrier might be disrupted[38] and oral administration of atorvastatin is considered to affect the brain directly.[39] The present findings suggest that orally administered atorvastatin crosses the blood–brain barrier and affects the brain of SHRSP. The abnormal activation of sympathetic nervous system causes hypertension, heart failure, and ischemic heart diseases, and we consider that oral administration of atorvastatin has a potential to treat cardiovascular diseases due to the sympathoinhibition through the antioxidant effect in the RVLM.

We previously demonstrated that oral administration of atorvastatin increases the expression of endothelial nitric oxide synthase (eNOS) in the brainstem.[40] Overexpression of eNOS in the RVLM decreases SNA in WKY and SHRSP.[26–28] In the present study, we did not investigate whether an increase in NO production in the RVLM is involved in the reduction of BP and oxidative stress. It is possible, however, that ICV injection of atorvastatin increases eNOS in the RVLM of SHRSP and that an increase in eNOS contributes to the sympathoinhibitory effect. Further study is needed to clarify this issue.

In WKY rats, atorvastatin does not alter SNA and oxidative stress in the RVLM; these results are compatible with our previous report.[7] Moreover, atorvastatin also does not alter Rac1-induced NAD(P)H oxidase activity and Mn-SOD activity in the RVLM of WKY rats. In the present study, the mechanisms by which atorvastatin affected Rac1-induced NAD(P)H oxidase activity and Mn-SOD activity in SHRSP, but not in WKY, were not determined. It may be that there are thresholds for the induction of Rac1-induced NAD(P)H oxidase activity and Mn-SOD activity in the RVLM, which

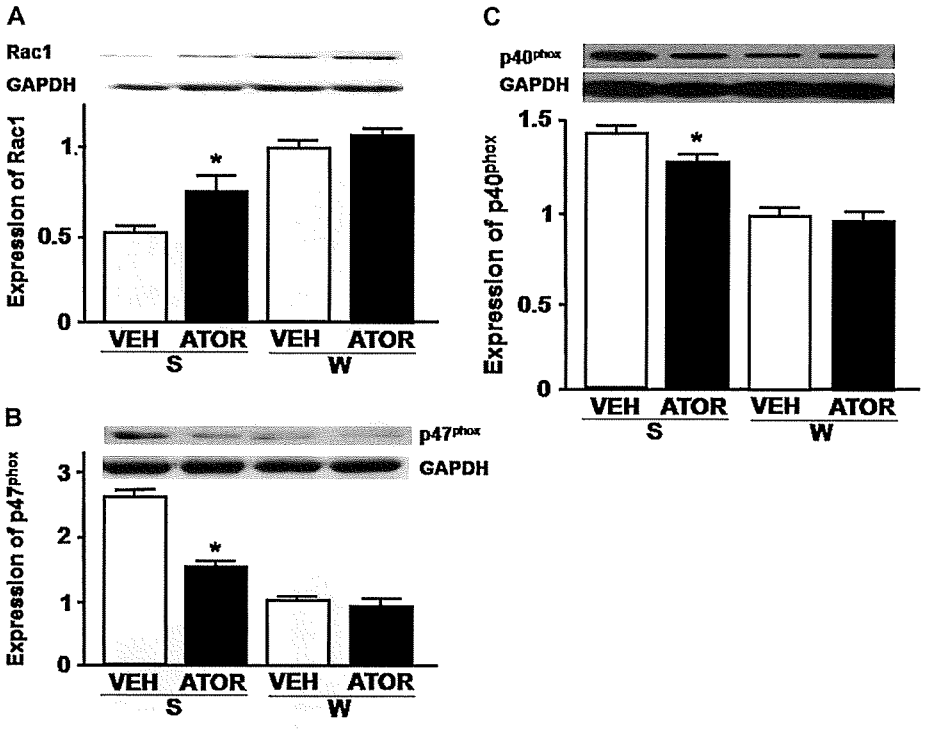

FIGURE 5. Western blot analysis showing the level of expression of Rac1 (A), $p47^{phox}$ (B), and $p40^{phox}$ (C) in the cytosolic fraction of the RVLM at day 14 in ATOR- or VEH-treated SHRSP or WKY (n = 5 per group). $*P < 0.05$ for ATOR versus VEH in each strain. $\dagger P < 0.05$ compared with VEH-treated WKY. The expression level of Rac1, $p47^{phox}$, and $p40^{phox}$ was expressed relative to that in W-VEH, which was assigned a value of 1. Data are shown as mean ± standard error of the mean.

are differently affected by atorvastatin between SHRSP and WKY rats.

STUDY LIMITATIONS

The present study has several limitations. First, we examined the effects of atorvastatin specifically in only the RVLM, and its effects in other brain areas cannot be excluded at this time. Nevertheless, neural activity in the RVLM has a direct influence on SNA,[1,2] and the present results identified an antioxidant effect of atorvastatin and its mechanisms in the RVLM. Angiotensin II type 1 receptors (AT_1R) are abundantly distributed in the RVLM, and there is a close link between AT_1R stimulation and NAD(P)H oxidase activation.[41] Therefore, in the present study, we focused on the RVLM, although other brain regions related to central autonomic control also contain AT_1R and NAD(P)H oxidase. Second, among all statins, we only studied the effect of atorvastatin, which is a lipophilic statin.[42] Our previous studies suggested that oral atorvastatin also reduces oxidative stress in the RVLM.[7] Further study is needed to clarify whether our results in the present study are broad class effects or are specific for atorvastatin. Finally, a recent study suggests that statins reduce BP in patients with hypertension.[43] It will be important to determine whether atorvastatin has this beneficial effect caused by the mechanism related to our suggestion in the present study, although we understand that this is difficult to examine in humans.

CONCLUSIONS

In conclusion, atorvastatin administered directly into the brain of SHRSP decreases BP, SNA, and baroreflex function. The findings of the present study suggest that these effects are associated with inhibition of oxidative stress in the RVLM, probably resulting from a decrease in NAD(P)H oxidase activity and the upregulation of Mn-SOD activity in the RVLM.

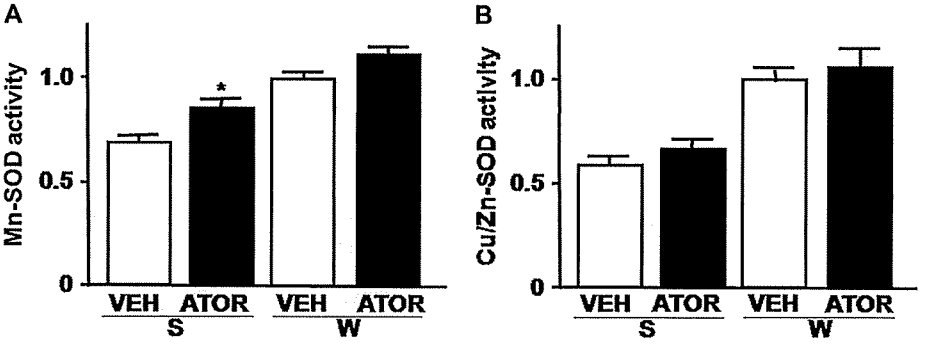

FIGURE 6. The activities of Mn-SOD (A) and Cu/Zn-SOD (B) in the RVLM at day 14 in ATOR- or VEH-treated SHRSP or WKY (n = 5 for each). $*P < 0.05$ for ATOR versus VEH in each strain. $\dagger P < 0.05$ compared with VEH-treated WKY. The activities of Mn-SOD and Cu/Zn-SOD were expressed relative to that in W-VEH, which was assigned a value of 1. Data are shown as mean ± standard error of the mean.

ACKNOWLEDGMENTS

We are grateful to Pfizer, Inc for supplying atorvastatin.

REFERENCES

1. Dampney RAL. Functional organization of central pathways regulating the cardiovascular system. *Physiol Rev.* 1994;74:323–364.
2. Guyenet PG. The sympathetic control of blood pressure. *Nat Rev Neurosci.* 2006;7:335–346.
3. Kishi T, Hirooka Y, Kimura Y, et al. Increased reactive oxygen species in rostral ventrolateral medulla contribute to neural mechanisms of hypertension in stroke-prone spontaneously hypertensive rats. *Circulation.* 2004;109:2357–2362.
4. Peterson JR, Sharma RV, Davisson RL. Reactive oxygen species in the neuropathogenesis of hypertension. *Curr Hypertens Rep.* 2006;8:232–241.
5. Hirooka Y. Role of reactive oxygen species in brainstem in neural mechanisms of hypertension. *Auton Neurosci.* 2008;142:20–24.
6. Sheh YL, Hsu C, Chan SHH, et al. NADPH oxidase- and mitochondrion-derived superoxide at rostral ventrolateral medulla in endotoxin-induced cardiovascular depression. *Free Radic Biol Med.* 2007;42:1610–1623.
7. Kishi T, Hirooka Y, Shimokawa H, et al. Atorvastatin reduces oxidative stress in the rostral ventrolateral medulla of stroke-prone spontaneously hypertensive rats. *Clin Exp Hypertens.* 2008;30:3–11.
8. Pliquett RU, Cornish KG, Peuler JD, et al. Simvastatin normalizes autonomic neural control in experimental heart failure. *Circulation.* 2003; 107:2493–2498.
9. Gao L, Wang W, Li YL, et al. Simvastatin therapy normalizes sympathetic neural control in experimental heart failure: roles of angiotensin II type 1 receptors and NAD(P)H oxidase. *Circulation.* 2005;112:1763–1770.
10. Gao L, Wang W, Zucker IH. Simvastatin inhibits central sympathetic outflow in heart failure by a nitric-oxide synthase mechanism. *J Pharmacol Exp Ther.* 2008;326:278–285.
11. Zimmerman MC, Dunlay RP, Lazartigues E, et al. Requirement for Rac1-dependent NADPH oxidase in the cardiovascular and dipsogenic actions of angiotensin II in the brain. *Circ Res.* 2004;95:532–539.
12. Nozoe M, Hirooka Y, Koga Y, et al. Inhibition of Rac1-derived reactive oxygen species in NTS decreases blood pressure and heart rate in stroke-prone SHR. *Hypertension.* 2007;50:62–68.
13. Byrne JA, Grieve DJ, Bendall JK, et al. Contrasting roles of NADPH oxidase isoforms in pressure-overload versus angiotensin II-induced cardiac hypertrophy. *Circ Res.* 2003;93:802–805.
14. Privratsky JR, Wold LE, Sowers JR, et al. AT1 blockade prevents glucose-induced cardiac dysfunction in ventricular myocytes: role of the AT1 receptor and NADPH oxidase. *Hypertension.* 2003;42:206–212.
15. Maach C, Kartes T, Killer H. Oxygen free radical release in human failing myocardium is associated with increased activity of Rac1-GTPase and represents a target for statin treatment. *Circulation.* 2003;108:1567–1574.
16. Wassmann S, Laufs U, Muller K, et al. Cellular antioxidant effects of atorvastatin in vitro and in vivo. *Arterioscler Thromb Vasc Biol.* 2002;22: 300–305.
17. Riad A, Du J, Stiehl S, et al. Low-dose treatment with atorvastatin leads to anti-oxidative and anti-inflammatory effects in diabetes mellitus. *Eur J Pharmacol.* 2007;569:204–211.
18. Habibi J, Whaley-Connell A, Qazi MA, et al. Rosuvastatin, a 3-hydroxy-3-methylglutaryl coenzyme A reductase inhibitor, decreases cardiac oxidative stress and remodeling in Ren2 transgenic rats. *Endocrinology.* 2007;148:2181–2188.
19. Whaley-Connell A, Habibi J, Nistala R, et al. Attenuation of NADPH oxidase activation and glomerular filtration barrier remodeling with statin treatment. *Hypertension.* 2008;51:474–480.
20. Chen X, Touyz RM, Park JB, et al. Antioxidant effects of vitamin C and E are associated with altered activation of vascular NADPH oxidase and superoxide dismutase in stroke-prone SHR. *Hypertension.* 2001;38: 606–611.
21. Carneado J, Alvarez de Sotomayor M, Perez-Guerrero C, et al. Simvastatin improves endothelial function in spontaneously hypertensive rats through a superoxide dismutase mediated antioxidant effect. *J Hypertens.* 2002;20:429–437.
22. Yilmaz MI, Baykal Y, Kilic M, et al. Effects of statins on oxidative stress. *Biol Trace Elem Res.* 2004;98:119–127.
23. Umeji K, Umemoto S, Itoh S, et al. Comparative effects of pitavastatin and probucol on oxidative stress, Cu/Zn superoxide dismutase, PPAR-gamma, and aortic stiffness in hypercholesterolemia. *Am J Physiol.* 2006;291: H2522–H2532.
24. Nozoe M, Hirooka Y, Koga Y, et al. Mitochondria-derived reactive oxygen species mediate sympathoexcitation induced by angiotensin II in the rostral ventrolateral medulla. *J Hypertens.* 2008;26:2176–2184.
25. Nishimura M, Takahashi H, Yoshimura M. Upregulation of the brain renin-angiotensin system in rats with chronic renal failure. *Acta Physiol (Oxf).* 2007;189:369–377.
26. Kishi T, Hirooka Y, Sakai K, et al. Overexpression of eNOS in the RVLM causes hypotension and bradycardia via GABA release. *Hypertension.* 2001;38:896–901.
27. Kishi T, Hirooka Y, Ito K, et al. Cardiovascular effects of overexpression of endothelial nitric oxide synthase in the rostral ventrolateral medulla in stroke-prone spontaneously hypertensive rats. *Hypertension.* 2002;39: 264–268.
28. Kishi T, Hirooka Y, Kimura Y, et al. Overexpression of eNOS in RVLM improves impaired baroreflex control of heart rate in SHRSP. *Hypertension.* 2003;41:255–260.
29. Castiglioni P, Di Rienzo M, Veicsteinas A, et al. Mechanisms of blood pressure and heart rate variability: an insight from low-level paraplegia. *Am J Physiol.* 2007;292:R1502–R1509.
30. Cerutti C, Gustin MP, Paultre CZ. Autonomic nervous system and cardiovascular variability in rats: a spectral analysis approach. *Am J Physiol.* 1991;261:H1292–H1299.
31. Pagani M, Montano N, Porta A, et al. Relationship between spectral components of cardiovascular variabilities, and direct measures of muscle sympathetic nerve activity in humans. *Circulation.* 1997;95:1441–1448.
32. Waki H, Kasparov S, Wong LF, et al. Chronic inhibition of eNOS activity in nucleus tractus solitarii enhances baroreceptor reflex in conscious rats. *J Physiol.* 2003;546:233–242.
33. Waki H, Katahira K, Polson JW, et al. Automation of analysis of cardiovascular autonomic function from chronic measurements of arterial pressure in conscious rats. *Exp Physiol.* 2006;91:201–213.
34. Braga VA, Burmeister MA, Sharma RV, et al. Cardiovascular responses to peripheral chemoreflex activation and comparison of different methods to evaluate baroreflex gain in conscious mice using telemetry. *Am J Physiol.* 2008;295:R1168–R1174.
35. Tai MH, Wang LL, Wu KL, et al. Increased superoxide anion in rostral ventrolateral medulla contributes to hypertension in spontaneously hypertensive rats via interactions with nitric oxide. *Free Radic Biol Med.* 2005;38:450–462.
36. Tanaka M, Umemoto S, Kawahara S, et al. Angiotensin II type 1 receptor antagonist and angiotensin-converting enzyme inhibitor altered the activation of Cu/Zn-containing superoxide dismutase in the heart of stroke-prone spontaneously hypertensive rats. *Hypertens Res.* 2005;28: 67–77.
37. Romero RM, Canuelo A, Lara EM, et al. Aging affects but does not eliminate the enzymatic antioxidative response to hypoxia/reoxygenation in cerebral cortex. *Exp Gerontol.* 2006;41:25–31.
38. Iwanaga Y, Ueno M, Ueki M, et al. The expression of osteopontin is increased in vessels with blood-brain barrier impairment. *Neuropathol Appl Neurobiol.* 2008;34:145–154.
39. Cibickova L, Radomir H, Stanislav M, et al. The influence of simvastatin, atorvastatin and high-cholesterol diet on acetylcholinesterase activity, amyloid beta and cholesterol synthesis in rat brain. *Steroids.* 2009;74: 13–19.
40. Kishi T, Hirooka Y, Mukai Y, et al. Atorvastatin causes depressor and sympatho-inhibitory effects with upregulation of nitric oxide synthases in stroke-prone spontaneously hypertensive rats. *J Hypertens.* 2003;21: 379–386.
41. Hu L, Zhu DN, Yu Z, et al. Expression of angiotensin II type 1 (AT1) receptor in the rostral ventrolateral medulla in rats. *J Appl Physiol.* 2002; 92:2153–2161.
42. Cibickova L, Hyspler R, Ticha A, et al. Cholesterol synthesis in central nervous system of rat is affected by simvastatin as well as by atorvastatin. *Pharmazie.* 2008;63:819–822.
43. Golomb BA, Dimsdale JE, White HL, et al. Reduction in blood pressure with statins: results from the USCD Statin Study, a randomized trial. *Arch Intern Med.* 2008;168:721–727.

J Physiol Sci (2010) 60:67–74
DOI 10.1007/s12576-009-0071-5

ORIGINAL PAPER

Effect of the cholinesterase inhibitor donepezil on cardiac remodeling and autonomic balance in rats with heart failure

Yoshihisa Okazaki · Can Zheng · Meihua Li · Masaru Sugimachi

Received: 28 July 2009 / Accepted: 4 November 2009 / Published online: 1 December 2009

Abstract In an earlier study we demonstrated the beneficial effect of direct vagal electrical stimulation on cardiac remodeling and survival. In the study reported here, we attempted to reproduce the effect of vagal enhancement through the administration of an acetylcholinesterase inhibitor, donepezil. A rat model of heart failure following extensive healed myocardial infarction was used. Compared to their nontreated counterparts, rats given donepezil (5 mg/kg/day) in their drinking water had a smaller biventricular weight (3.40 ± 0.13 vs. 3.02 ± 0.21 g/kg body weight, $P < 0.05$), and maximal rate of rise (3256 ± 955 vs. 3822 ± 389 mmHg/s, $P < 0.05$) and the end-diastolic value (30.1 ± 5.6 vs. 23.2 ± 5.7 mmHg, $P < 0.05$) of left ventricular pressure were improved. Neurohumoral factors were suppressed in donepezil-treated rats (norepinephrine 1885 ± 1423 vs. 316 ± 248 pg/ml, $P < 0.01$; brain natriuretic peptide 457 ± 68 vs. 362 ± 80 ng/ml, $P < 0.05$), and the high-frequency component of heart rate variability showed a nocturnal increase. These findings indicated that donepezil reproduced the anti-remodeling effect of electrical vagal stimulation. Further studies are warranted to evaluate the clinical usefulness of donepezil in heart failure.

Y. Okazaki · M. Sugimachi
Department of Artificial Organ Medicine, Division of Surgical Medicine, Osaka University Graduate School of Medicine, 2-2 Yamadaoka, Suita, Osaka 565-0871, Japan

Y. Okazaki · C. Zheng · M. Li · M. Sugimachi (✉)
Department of Cardiovascular Dynamics, Advanced Medical Engineering Center, National Cardiovascular Center Research Institute, 5-7-1 Fujishirodai, Suita, Osaka 565-8565, Japan
e-mail: su91mach@ri.ncvc.go.jp

Keywords Heart rate variability · Myocardial infarction · Neurohumoral activation · Vagal stimulation

Introduction

Profound imbalances in the autonomic nervous system, such as overactive sympathetic activity as well as diminished vagal activity, are considered to be important factors that aggravate heart failure [1, 2]. Various therapeutic agents, including beta-blockers [3, 4], angiotensin converting enzyme inhibitors [5, 6], and angiotensin receptor antagonists [7, 8] have proven to be useful pharmacotherapy, not a little by correcting the abnormally augmented sympathetic activity. However, few attempts have been made to date to actively remedy the reduced vagal activity as a treatment for heart failure. As a first attempt to testing this therapeutic strategy, our group has shown that in rats with aggravating chronic heart failure after experimentally induced healed myocardial infarction, electrical stimulation of the vagus nerve markedly improved survival by preventing cardiac remodeling [9].

Since the efferent vagal nerve activity is transmitted by acetylcholine, drugs that increase acetylcholine concentration at the neuro-effector junction are expected to have an effect similar to that of electrical stimulation. In support of this hypothesis, clinical trials in which patients with chronic heart failure were treated with the acetylcholinesterase inhibitor pyridostigmine reported decreased ventricular arrhythmia, enhanced heart rate variability at rest, increased heart rate reserve and oxygen pulse during exercise, and improved heart rate recovery after exercise [10, 11]. However, these studies examined the effect of short-term administration (1–2 days), and to date the long-term effect of pyridostigmine has not been investigated.

Clinical trials have also been conducted on scopolamine, which stimulates vagus nerve centrally at low doses [12, 13]. Transdermal administration of a small dose of scopolamine in patients with heart failure following myocardial infarction was found to increase heart rate variability and enhance baroreflex sensitivity. These studies have not shown, however, an anti-remodeling effect as more direct evidence against the progression of heart failure.

We hypothesized that donepezil, a novel acetylcholinesterase inhibitor, would show various clinically relevant beneficial effects through its preferential effects on neural true cholinesterase (rather than hepatic pseudocholinesterase) [14]. Therefore, in the study reported here, we investigated the effect of donepezil on hemodynamics, neurohumoral activation, and cardiac remodeling in rats with chronic heart failure. We also analyzed the high-frequency (HF) component of the heart rate variability to assess changes in vagal tone [15, 16]. Our results suggest that donepezil reproduces the anti-remodeling effect of electrical stimulation of the vagus nerve and increases vagal tone.

Materials and methods

The protocol of this study was performed in accordance with the Guiding Principles for the Care and Use of Animals in the Field of Physiological Sciences and was approved by the Experimental Animal Committee of the National Cardiovascular Center.

Chronic heart failure model

Male Sprague–Dawley rats (8 weeks of age) were used. A thoracotomy was performed under halothane anesthesia, and the main branch of the left coronary artery was ligated with nylon to produce myocardial infarction. The ligation resulted in myocardial infarction of 45–55%. The rats recovered from this extensive myocardial infarction and progressed to the chronic state of heart failure (see Results). The ventricular fibrillation that occurred within 1 h of ligation was treated actively by defibrillation and cardiac massage in order to salvage as many as possible rats with extensive myocardial infarction.

Experimental protocol

One week after the induction of myocardial infarction, the surviving rats underwent a second operation under halothane anesthesia in which an electrocardiogram (ECG) telemetry device was implanted in each rat to continuously monitor the electrical activity of the heart and heart rate (Fig. 1a).

Rats that survived the second week were divided into a nontreated group and a donepezil group. The donepezil group was administered the acetylcholinesterase inhibitor

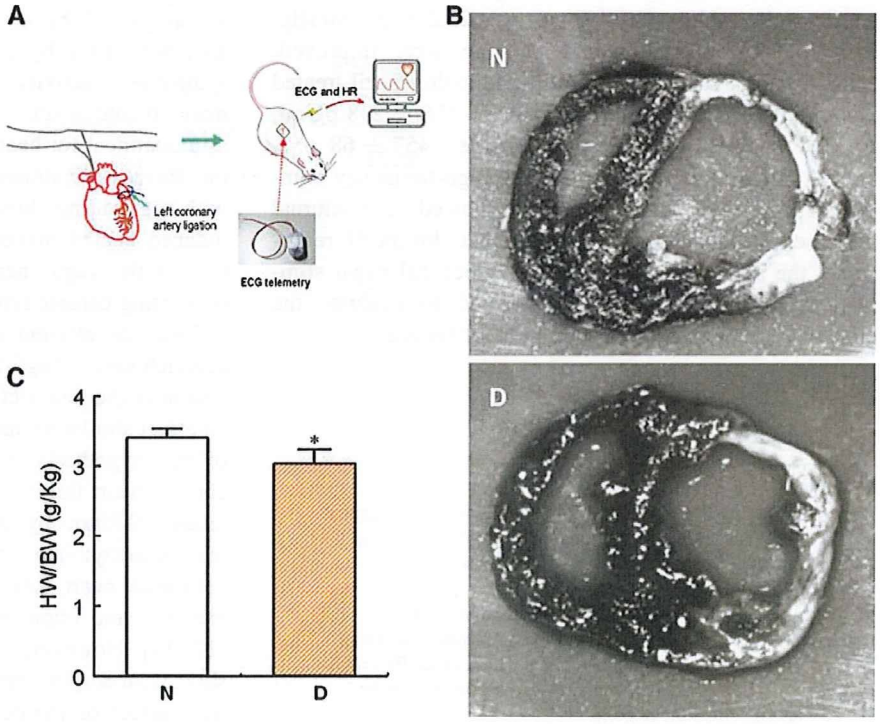

Fig. 1 **a** Schematic representation of the experimental design. Electrocardiogram (*ECG*) was recorded continuously using a telemetric system. **b** Ventricular sections of representative animals at week 6 of treatment (8 weeks post-infarction). No significant difference in the size of the myocardial infarction was observed between the donepezil group and the nontreated group. Compared with the nontreated heart (*N*), the donepezil-treated heart (*D*) had a thicker scar in the infarct area with more spared myocardium in the border area. **c** Combined weight of left and right ventricles per body weight (*HW/BW*) at week 6 of treatment. Ventricular weight was significantly lower ($*P < 0.05$) in the donepezil group (*shaded bar*, *D*) than in the nontreated group (*open bar*, *N*)

donepezil (Aricept; Eisai, Tokyo, Japan) dissolved in drinking water at a concentration of 50 mg/dl. The dose estimated from the volume of water consumed was 5 mg/kg/day on average. The selection of donepezil rested on the fact that, in comparison to other drugs, its inhibition action is directed much more towards the (true) acetylcholinesterase at synapses and effectors and less towards pseudocholinesterase (butyrylcholinesterase) in the liver [14].

At week 6 post-treatment (week 8 after infarction was induced), 13 rats in the nontreated group and 14 rats in the donepezil group were subjected to a hemodynamic study under halothane anesthesia. Following this study and blood collection, the rats were euthanized by an overdose of halothane, and a histological examination was conducted.

In 11 other rats with a similar healed myocardial infarction, the heart rate variability was calculated from the continuous ECG recordings between weeks 12 and 20 post-myocardial infarction induction. Five of these 11 rats served as the nontreated group (weeks 12–20 post-infarction), and six received the donepezil treatment (weeks 17–19 post-infarction). Preliminary analysis indicated no differences in heart rate variability at 8 weeks post-infarction.

Hemodynamic measurement

The hemodynamic study was conducted in rats under halothane anesthesia at week 6 of the treatment period. A Millar catheter (SPC-320; Millar Instruments, Houston, TX) was inserted from the carotid artery into the left ventricle to measure left ventricular pressure (LVP) with a high-fidelity catheter. Based on the LVPs, we calculated the maximal first derivative of left ventricular pressure over time (dP/dt_{max}) and the left ventricular end-diastolic pressure (LVEDP). The right atrial pressure (RAP) was measured by an external transducer via a catheter filled with physiological saline.

Neurohumoral factor measurements

Blood samples (3 ml) were collected and the neurohumoral factors in the blood assayed. As indices of sympathetic activity, norepinephrine (NE) and epinephrine (Epi) were measured by high-performance liquid chromatography with electrochemical detection. The plasma level of brain (or B-type) natriuretic peptide (BNP) was measured by an enzyme-linked immunosorbent (ELISA) assay (BNP-32 Enzyme Immunoassay kit, Peninsula Lab, San Carlos, CA). We included BNP in the assay due to its importance as a strong predictor of prognosis [17, 18]. BNP has been useful in detecting new patients with heart failure and in predicting mortality and cardiac events in both patients and asymptomatic subjects. BNP may also be a useful predictor of heart failure with preserved systolic function.

Heart tissue examination

The left and right ventricles were excised and the total weight measured. Both ventricles were then sectioned into 3-mm-thick slices, starting from the apex towards the base of the heart. Myocardial infarction size was assessed from the proportion of the length of the infarct to the left ventricular perimeter measured on each section.

Power spectral analysis of heart rate variability

The ECG telemetric data were processed as follows. Signals from the transmitter (model TA11CTA-F40; Data Sciences Int, St. Paul, MN) were recorded on a recording software (HEM; Notocord, Newark, NJ). An analysis software program (HRT10a1; Notocord) was used to extract the RR intervals from the data of the continuous recording (1-kHz sampling). All of the RR intervals were extracted from 24-h continuous recording data for the nontreated and the donepezil groups. The text data of 2-h intervals were stored in files to be analyzed later using the heart rate variability analysis software that we developed. Due to the frequent occurrence of extrasystoles in chronic heart failure, it was necessary to develop an original algorithm to process the data, as explained below.

Heart rate variability analysis software

The following procedures were conducted.

1. Data preparation. The 2-h data were combined to obtain 24-h data. The time of R-wave detection and the RR interval were saved as combined data.
2. Removal of extrasystole. A 20-point median filter was applied to all of the RR interval data to produce a sequence. Heart beats with RR intervals differing from the median value by 15 ms (threshold) or above were recognized and recorded as extrasystole or post-extrasystole. These data were excluded from analysis.
3. Resampling of valid interval data. The 24-h data were divided into 6-min data (with 50% overlap). After excluding the RR intervals associated with extrasystole, the valid RR interval data were resampled at intervals of 1/10 s using linear interpolation.
4. Power spectral analysis. In the power spectral analysis, 1024 points of 1/10-s data were grouped into a segment (segment length = 102.4 s) for fast Fourier transformation (FFT). The power spectra obtained from six segments were ensemble-averaged. Prior to FFT, the linear trend was removed from each segment
5. Data selection. Even though extrasystoles are removed, segments with many deleted data cannot be expected to yield reliable power spectral analysis results. Therefore,

data with ≥40 extrasystoles within 6 min were excluded from analysis.

6. Definition of HF component. In this study, the effect of bigeminy that occurs in heart failure was observed in the higher frequency range. Therefore, we excluded frequency range >1.5 Hz, and HF was defined as the power from 0.5 to 1.5 Hz. The power of the HF component was determined during daytime (0600–1800 hours) and nighttime (1800–0600 hours).

Statistical analysis

All data are presented as mean ± standard deviation (SD). Continuous variables were compared using the unpaired *t* test between two groups. The differences were considered significant when $P < 0.05$.

Results

Hemodynamics

Figure 2 shows the measurements of the hemodynamic parameters in rats under anesthesia 6 weeks after the onset of donepezil administration. A LVP waveform and its first derivative (dP/dt) in a nontreated rat are shown in Fig. 2a. Figure 2b shows that the dP/dt_{max} of the nontreated rat was significantly lower than that of the donepezil group (3,256 ± 955 vs. 3,822 ± 389 mmHg/s, $P < 0.05$). The LVEDP and RAP was significantly lowered by donepezil administration compared to the nontreated rat [23.2 ± 5.7 vs. 30.1 ± 5.6 mmHg, $P < 0.05$ (Fig. 2c) and 4.1 ± 2.9 vs. 7.0 ± 4.0 mmHg, $P < 0.05$ (Fig. 2d), respectively]. The contractility index dP/dt_{max} is known as a heart rate-

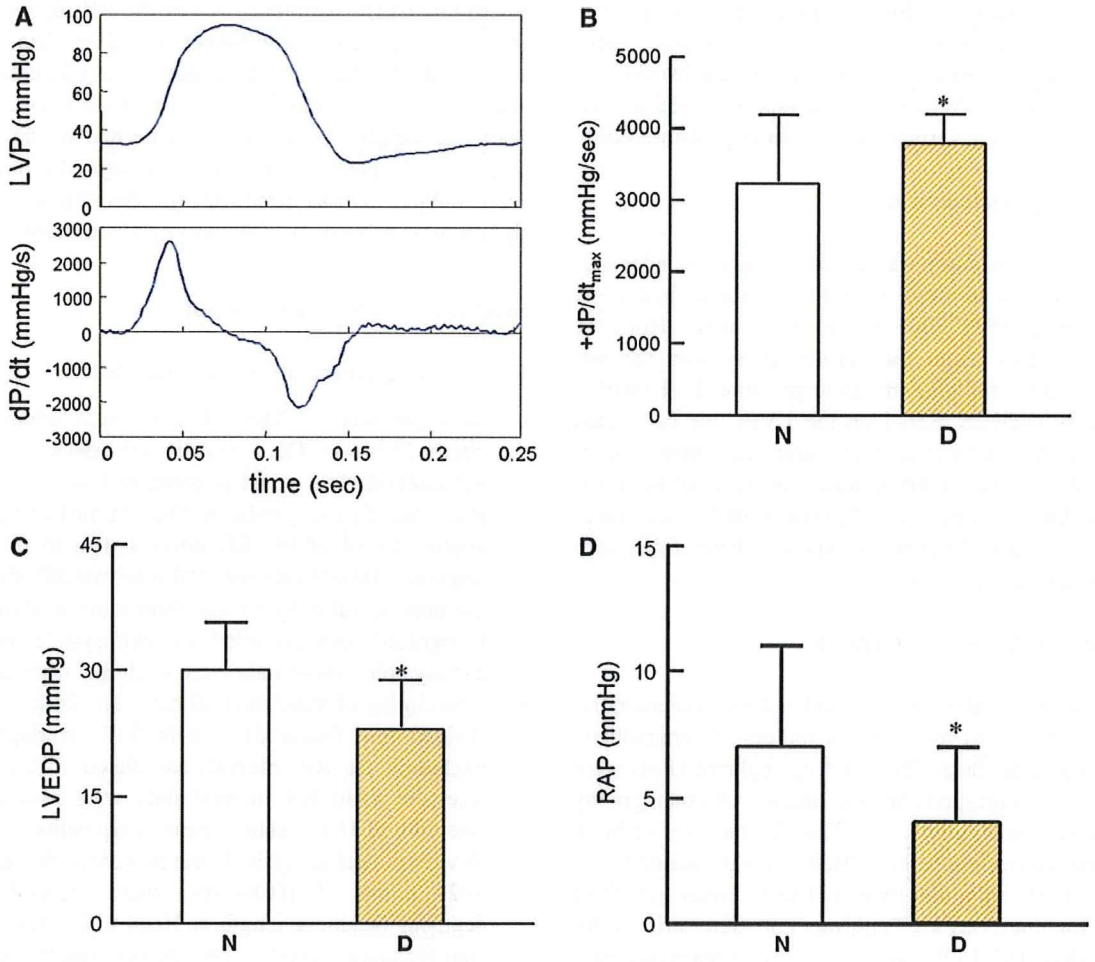

Fig. 2 **a** A representative example of the left ventricular pressure (*LVP*) waveform and its derivative in a nontreated rat. **b** Maximal first derivative of left ventricular pressure (dP/dt_{max}) at week 6 of treatment. The dP/dt_{max} was significantly ($^*P < 0.05$) higher in the donepezil group (*shaded bar*, *D*) than in the nontreated group (*open bar*, *N*). **c** Left ventricular end-diastolic pressure (*LVEDP*) at week 6 of treatment. The LVEDP was significantly lower in the donepezil group (*shaded bar*, *D*) than in the nontreated control group (*open bar*, *N*). **d** Right atrial pressure (*RAP*) at week 6 of treatment. The RAP was significantly ($^*P < 0.05$) lower in the donepezil group (*shaded bar*, *D*) than in the nontreated control group (*open bar*, *N*)

and preload-dependent index. Because heart rate was higher in the nontreated group than in the donepezil group (354 ± 37 vs. 324 ± 23 bpm, difference of approx. 9%) and LVEDP was higher in the nontreated group than in the donepezil group, the difference in heart rate and preload would have underestimated the true difference in contractility. Moreover, decreased LVEDP with decreased RAP in the donepezil group suggested that body fluid retention was suppressed.

Neurohumoral factors

Figure 3 shows the blood concentrations of norepinephrine, epinephrine, and BNP measured 6 weeks after donepezil administration was started. Compared to the nontreated group, donepezil administration resulted in significant decreases in the concentrations of norepinephrine (316 ± 248 vs. 1,885 ± 1423 pg/ml, $P < 0.01$), epinephrine (347 ± 153 vs. 1,694 ± 1,355 pg/ml, $P < 0.05$), and BNP (362 ± 80 vs. 457 ± 68 ng/ml, $P < 0.05$) in the blood. These results indicated that donepezil effectively suppressed the overactive sympathetic nervous system, which is a hallmark pathophysiology of heart failure.

Infarct size and heart weight

Figure 1b shows representative ventricular sections in the nontreated and the donepezil groups. The myocardial infarction resulted from obliteration of the left coronary artery was 48 ± 6% of the left ventricular perimeter in the nontreated group and 53 ± 3% in the donepezil group, with no significant difference in infarct size between two groups. Therefore, donepezil administration started 2 weeks after myocardial infarction did not reduce the size of the infarct, suggesting that infarct size did not account for the differences in hemodynamics and neurohumoral factors described above.

Figure 1c compares the ventricular weight per body weight between the nontreated and the donepezil groups. The combined weight of the left and right ventricles was significantly lower in the donepezil group than in the nontreated group (3.02 ± 0.21 vs. 3.40 ± 0.13 g/kg body weight, $P < 0.05$). This result indicated that donepezil reduced cardiac remodeling after myocardial infarction was completed.

Power spectral analysis of heart rate variability

The left panel of Fig. 4a shows a representative change in RR intervals with respect to time in a rat from the donepezil group. The RR intervals connected with dotted lines were assessed to be extrasystoles or post-extrasystoles and were removed before spectral analysis. The right panel shows the result of spectral analysis from the same data. The solid area was calculated as the HF component. The HF components during the daytime (0600–1800 hours, Fig. 4b) and nighttime (1800–0600 hours, Fig. 4c) were calculated for the donepezil group ($n = 6$) and the nontreated group ($n = 5$). The log-transformed HF components [log(HF)] of the two groups were analyzed statistically.

During the night, log(HF) significantly increased in the donepezil group compared to the untreated group. On the other hand, there was no significant difference in log(HF) during the day between the two groups. These results indicated that heart rate variability at night was enhanced by donepezil administration in rats.

Discussion

Imbalances in the autonomic nervous system, particularly overactive sympathetic activity together with reduced

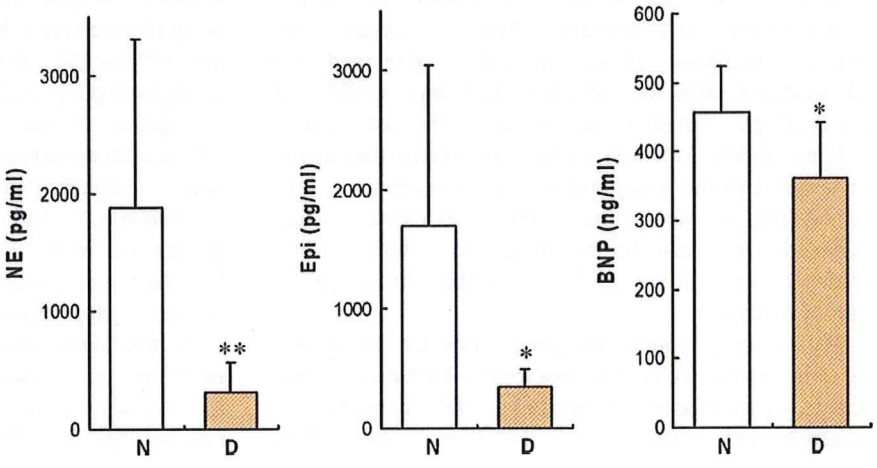

Fig. 3 Blood concentrations of norepinephrine (*NE*), epinephrine (*Epi*), and brain natriuretic peptide (*BNP*) at week 6 of treatment. Significant decreases (*$P < 0.05$, **$P < 0.01$) in blood NE, Epi, and BNP concentrations were observed in the donepezil group (*shaded bar*, *D*) compared to the nontreated group (*open bar*, *N*)

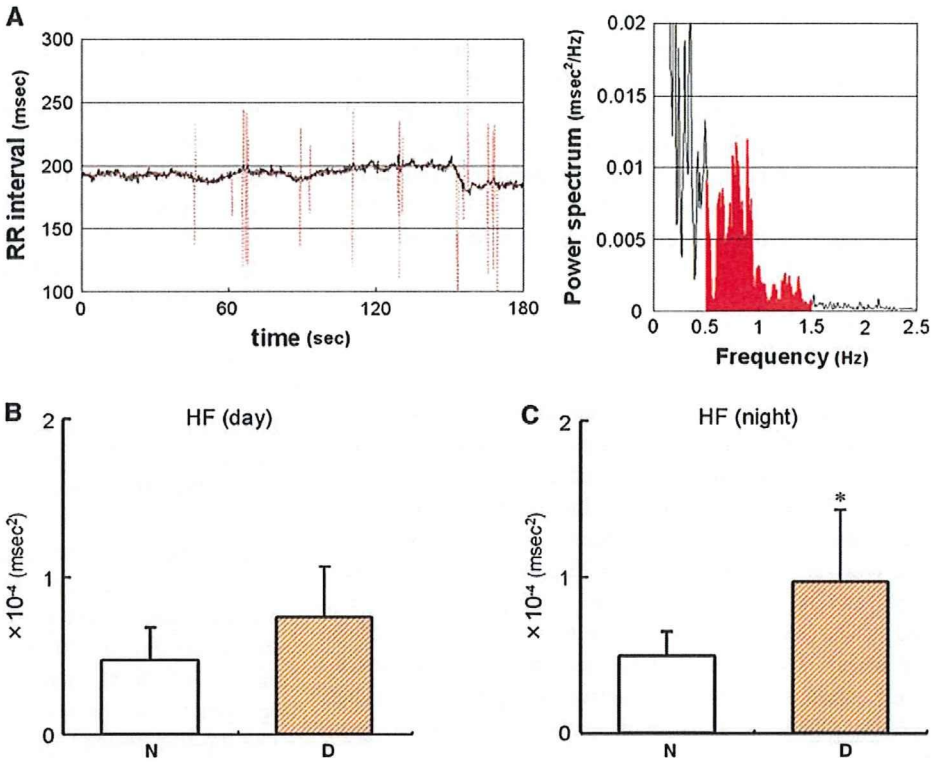

Fig. 4 **a** A representative example of time series of RR interval (*left*) and its power spectrum (*right*) in a donepezil-treated rat. RR intervals shown with *dotted lines* were assessed to be extrasystoles or post-extrasystoles and were removed before the power spectrum was calculated. *Solid area* indicates the high-frequency (HF) component. **b** HF of heart rate variability during the day. No significant difference in daytime HF value was observed between the donepezil group (*shaded bar*, *D*) and the nontreated group (*open bar*, *N*). **c** HF component of heart rate variability during the night. The nocturnal HF value of the donepezil group (*shaded bar*, *D*) was significantly higher than that of the nontreated group (*open bar*, *N*). $*P < 0.05$ by *t* test using log(HF) values

vagal activity, have been considered to be major factors aggravating heart failure. In an earlier study, we demonstrated that upstream treatment using electrical stimulation of the vagal nerve improves the survival rate in rats with heart failure after a healed extensive myocardial infarction. Although pharmacological reproduction of the vagotonic treatment of heart failure would be of benefit clinically, no vagotonic drugs have successfully shown anti-remodeling, which is the most direct evidence of a lack of progression of heart failure.

The results presented here clearly demonstrate that, in our rat model system, donepezil treatment improved hemodynamics, ameliorated cardiac remodeling, and prevented neurohumoral activation. Because donepezil exerted no significant effects on infarct size and was administered after the infarction had been established, these effects cannot be attributed to the reduction in ischemic insult. Although we have not shown the benefits on survival in this study, the similar hemodynamic, anti-remodeling, and neurohumoral effects as electrical vagal stimulation may also be translated into survival. Further studies on survival are needed to test the clinical application of donepezil.

We did not prepare sham-operated rats that would serve as a true control. To compensate for this limitation in study design, we used historical control values for hemodynamic measurements (dP/dt_{max} 11,237 ± 1,389 mmHg/s, LVEDP 6.5 ± 2.3 mmHg; RAP 1.9 ± 1.3 mmHg), neurohumoral factor measurements (NE 392 ± 205 pg/ml, Epi 164 ± 46 pg/ml, BNP 62 ± 7 pg/ml), and biventricular weight (2.22 ± 0.11 g/kg) obtained from the same strain and similar age of rats. These control values indicate that hemodynamic deterioration, neurohumoral activation, and cardiac remodeling were only partially reversed, with the exception of NE. Notwithstanding, the results with the electrical stimulation of vagal nerves indicate that these small benefits may accompany a larger improvement in survival.

We selected donepezil, a novel cholinesterase inhibitor, in order to be able to maximize inhibitor action on neuronal acetylcholinesterase but not on hepatic butyrylchoinesterase inhibitor [14]. We intentionally used donepezil, a drug acting both peripherally and centrally, to simulate electrical stimulation of the vagus nerve. Electrical stimulation affects both the afferent and efferent pathways of the vagus nerve, although detailed knowledge of the therapeutic mechanisms, including which of the two pathways plays a greater role in the therapeutic effect, is not yet available. However, a drug with dual central and peripheral action is certainly inappropriate for deepening mechanistic insights.

A mechanistic study would be important as donepezil itself may not be clinically applicable. The dose we chose in our study was aimed at decreasing the heart rate in the rats by 10%; it is 50-fold larger than the dose used for

treating Alzheimer's disease. Although the objective of our study was not to elucidate how large the contribution of each effect of donepezil is on the peripheral vagus nerve, ganglion, and central nervous system, we would like to add discuss some mechanistic aspects in terms of designing future studies.

Regarding the mechanism downstream of the neuro-effector junction, the neurotransmitter acetylcholine per se may provide some protective effect for cardiomyocytes. Based on their results from acute studies, Sato et al. have obtained several lines of evidence supporting this hypothesis. First, acetylcholine promotes the phosphorylation of connexin 43, a gap junction molecule located between cardiomyocytes, which in turn normalizes the intercellular ion flow and prevents the occurrence of fatal arrhythmia [19]. Second, acetylcholine directly enhances the phosphorylation of Akt via PI3K in the cardiomyocytes and activates the PI3/Akt pathway to enhance the expression of hypoxia-inducible factor-1α (HIF-1α), which may protect the cardiomyocytes from the hypoxic state induced by ischemia [20]. As shown by these findings, the acetylcholine concentration increases in the neuro-effector junction by vagal efferent activation; this acetylcholine possesses various functions that support the survival of cardiomyocytes. Further studies are required to study the contribution of acetylcholine in cardiomyocytes at the molecular level. Vagal enhancement at the effector site may potentiate its anti-inflammation effects [21] and may ameliorate progression of heart failure through alpha 7-nicotinic receptors.

On the other hand, experiments using rat and canine models of heart failure suggest the presence of abnormalities in the ganglia of the vagus nerve. For example, a comparison of control rats to those with heart failure following myocardial infarction revealed that the bradycardiac response to pre-ganglionic vagus stimulation in the rats with infarction was attenuated, while the bradycardiac response to acetylcholine was unchanged [22]. In dogs with heart failure induced by tachypacing, pre-ganglionic vagus stimulation showed lower heart rate responses, while postganglionic stimulation at the fat pad showed no difference in heart rate response compared to control dogs [23]. Taken together the above observations, in our model system, donepezil may act on the ganglia of the vagus nerve.

As donepezil passes the blood–brain barrier, the drug can act on the central nervous system. To gain an insight into the central effect, we conducted an analysis of heart rate variability. Heart rate variability, especially its HF component (at respiratory frequency) reflects background vagal tone and has been shown to be a strong prognostic determinant [15, 16]. Our results revealed that donepezil increased the HF of heart rate variability during the night, indicating enhanced vagal activity. On the other hand, the HF of the heart rate variability tended to increase, although not significantly, during the day. These finding may suggest a central effect of donepezil, but again a secondary effect of improved hemodynamics cannot be ruled out. Regardless of the detailed mechanism, increased HF may be associated to a better outcome in these rats, as shown in the ATRAMI study [24, 25]. These issues require further investigations.

In summary, the results of the study reported here suggest that donepezil treatment, similar to electrical stimulation of the vagus nerve, confers beneficial effects in terms of the prevention of cardiac remodeling in rats with heart failure following myocardial infarction. Future studies should examine if survival would be improved by the administration of donepezil in rats with healed myocardial infarction.

Acknowledgments This study was supported by Health and Labor Sciences Research Grants (H19-nano-Ippan-009, H20-katsudo-Shitei-007) from the Ministry of Health, Labor and Welfare of Japan.

References

1. Packer M (1992) The neurohormonal hypothesis: a theory to explain the mechanism of disease progression in heart failure. J Am Coll Cardiol 20:248–254
2. Floras JS (1993) Clinical aspects of sympathetic activation and parasympathetic withdrawal in heart failure. J Am Coll Cardiol 22:72A–84A
3. Packer M, Bristow MR, Cohn JN, Colucci WS, Fowler MB, Gilbert EM, Shusterman NH, U.S. Carvedilol Heart Failure Study Group (1996) The effect of carvedilol on morbidity and mortality in patients with chronic heart failure. N Engl J Med 334:1349–1355
4. Bristow MR, Gilbert EM, Abraham WT, Adams KF, Fowler MB, Hershberger RE, Kubo SH, Narahara KA, Ingersoll H, Krueger S, Young S, Shusterman N, MOCHA Investigators (1996) Carvedilol produces dose-related improvements in left ventricular function and survival in subjects with chronic heart failure. Circulation 94:2807–2816
5. The CONSENSUS Trial Study Group (1987) Effects of enalapril on mortality in severe congestive heart failure. Results of the Cooperative North Scandinavian Enalapril Survival Study (CONSENSUS). N Engl J Med 316:1429–1435
6. The SOLVD Investigators (1991) Effect of enalapril on survival in patients with reduced left ventricular ejection fractions and congestive heart failure. N Engl J Med 325:293–302
7. Cohn JN, Tognoni G, Valsartan Heart Failure Trial Investigators (2001) A randomized trial of the angiotensin-receptor blocker valsartan in chronic heart failure. N Engl J Med 345:1667–1675
8. McMurray JJ, Ostergren J, Swedberg K, Granger CB, Held P, Michelson EL, Olofsson B, Yusuf S, Pfeffer MA, CHARM Investigators and Committees (2003) Effects of candesartan in patients with chronic heart failure and reduced left-ventricular systolic function taking angiotensin-converting-enzyme inhibitors: the CHARM-added trial. Lancet 362:767–771
9. Li M, Zheng C, Sato T, Kawada T, Sugimachi M, Sunagawa K (2004) Vagal nerve stimulation markedly improves long-term survival after chronic heart failure in rats. Circulation 109:120–124

10. Serra SM, Costa RV, Teixeira De Castro RR, Xavier SS, Lucas Da Nóbrega AC (2009) Cholinergic stimulation improves autonomic and hemodynamic profile during dynamic exercise in patients with heart failure. J Card Fail 15:124–129
11. Behling A, Moraes RS, Rohde LE, Ferlin EL, Nóbrega AC, Ribeiro JP (2003) Cholinergic stimulation with pyridostigmine reduces ventricular arrhythmia and enhances heart rate variability in heart failure. Am Heart J 146:494–500
12. Casadei B, Conway J, Forfar C, Sleight P (1996) Effect of low doses of scopolamine on RR interval variability, baroreflex sensitivity, and exercise performance in patients with chronic heart failure. Heart 75:274–280
13. Venkatesh G, Fallen EL, Kamath MV, Connolly S, Yusuf S (1996) Double blind placebo controlled trial of short term transdermal scopolamine on heart rate variability in patients with chronic heart failure. Heart 76:137–143
14. Liston DR, Nielsen JA, Villalobos A, Chapin D, Jones SB, Hubbard ST, Shalaby IA, Ramirez A, Nason D, White WF (2004) Pharmacology of selective acetylcholinesterase inhibitors: implications for use in Alzheimer's disease. Eur J Pharmacol 486:9–17
15. Kleiger RE, Miller JP, Bigger JT Jr, Moss AJ (1987) Decreased heart rate variability and its association with increased mortality after acute myocardial infarction. Am J Cardiol 59:256–262
16. Schwartz PJ, La Rovere MT (1998) ATRAMI: a mark in the quest for the prognostic value of autonomic markers. Autonomic tone and reflexes after myocardial infarction. Eur Heart J 19:1593–1595
17. Anand IS, Fisher LD, Chiang YT, Latini R, Masson S, Maggioni AP, Glazer RD, Tognoni G, Cohn JN, Val-HeFT Investigators (2003) Changes in brain natriuretic peptide and norepinephrine over time and mortality and morbidity in the Valsartan heart failure trial (Val-HeFT). Circulation 107:1278–1283
18. Doust JA, Pietrzak E, Dobson A, Glasziou P (2005) How well does B-type natriuretic peptide predict death and cardiac events in patients with heart failure: systematic review. Br Med J 330:625
19. Ando M, Katare RG, Kakinuma Y, Zhang D, Yamasaki F, Muramoto K, Sato T (2005) Efferent vagal nerve stimulation protects heart against ischemia-induced arrhythmias by preserving connexin 43 protein. Circulation 112:164–170
20. Kakinuma Y, Ando M, Kuwabara M, Katare RG, Okudela K, Kobayashi M, Sato T (2005) Acetylcholine from vagal stimulation protects cardiomyocytes against ischemia and hypoxia involving additive non-hypoxic induction of HIF-1alpha. FEBS Lett 579:2111–2118
21. Wang H, Yu M, Ochani M, Amella CA, Tanovic M, Susarla S, Li JH, Wang H, Yang H, Ulloa L, Al-Abed Y, Czura CJ, Tracey KJ (2003) Nicotinic acetylcholine receptor alpha7 subunit is an essential regulator of inflammation. Nature 421:384–388
22. Du XJ, Cox HS, Dart AM, Esler MD (1998) Depression of efferent parasympathetic control of heart rate in rats with myocardial infarction: effect of losartan. J Cardiovasc Pharmacol 31:937–944
23. Bibevski S, Dunlap ME (1999) Ganglionic mechanisms contribute to diminished vagal control in heart failure. Circulation 99:2958–2963
24. La Rovere MT, Bigger JT Jr, Marcus FI, Mortara A, Schwartz PJ (1998) Baroreflex sensitivity and heart-rate variability in prediction of total cardiac mortality after myocardial infarction ATRAMI (autonomic tone and reflexes after myocardial infarction) Investigators. Lancet 351:478–484
25. La Rovere MT, Pinna GD, Hohnloser SH, Marcus FI, Mortara A, Nohara R, Bigger JT Jr, Camm AJ, Schwartz PJ, ATRAMI Investigators (2001) Baroreflex sensitivity and heart rate variability in the identification of patients at risk for life-threatening arrhythmias: implications for clinical trials. Circulation 103:2072–2077